Mapping differential interactomes by affinity purification coupled with data independent mass spectrometry acquisition

Jean-Philippe Lambert, Gordana Ivosev, Amber L. Couzens, Brett Larsen, Mikko Taipale, Zhen-Yuan Lin, Quan Zhong, Susan Lindquist, Marc Vidal, Ruedi Aebersold, Tony Pawson, Ron Bonner, Stephen Tate* and Anne-Claude Gingras*

Please send correspondence to:
Stephen Tate, Stephen.Tate@absciex.com or Anne-Claude Gingras, gingras@lunenfeld.ca

List of Supplementary Tables and Figures

Note that these Supplementary materials are complemented by a website containing all larger files. Access the website at prohits-web.lunenfeld.ca.

Supplementary discussion

While our characterization of CDK4 cancer derived mutation focused on Arg24 mutants (R24C and R24H), we also tested the impact of other common CDK4 mutations. To do so, we also expressed two other cancer associated variants of CDK4, namely N41S and S52N, and characterized them as per **Fig. 1a**. All proteins were expressed at similar though not identical levels (CDK4 N41S levels being slightly elevated), as detected by immunoblotting (**Supplementary. Fig. 19b**). Mutation of N41S or S52N did not preclude association with the INK proteins, as determined by AP-SWATH and AP-western (**Supplementary. Fig. 19a, 20-22**). Most of the changes noted with sequence variants at R24 (including increased association with CDC37 and HSP90) were not observed with the S52N proteins that looked

most similar to the WT CDK4, while the N41S variant exhibited an intermediate phenotype (**Supplementary. Fig. 19a**, **20-22**)**.**

In addition to the point mutant samples presented in the main text, we also tested whether the approach was generally applicable to other types of sequence alterations, notably splice variants. We selected a series of splice variants of GRK6 (**Supplementary Fig. 29a**), a GPCR-associated kinase[1]: these splice variants were recently demonstrated to differentially interact with the chaperone HSP90[2]. While HSP90 was found to interact with all three GRK6 splice isoforms, AP-western showed a stronger interaction with the B splice variant (**Supplementary Fig. 29b**).

By using the pipeline shown in **Fig. 1a** on the GRK6 samples, we were able to measure global changes between proteins interacting with each of the three splice variants. Sets of proteins that differentially associated with each GRK6 splice variant were identified (**Supplementary. Fig. 29c-d**; **30-32**). While HSP90 showed increased interactions with the B splice variant, the Fold Changes were not significant after our statistical analysis. The levels of the kinase-specific CDC37 protein were also only mildly regulated across variants, however, the FKBP52 immunophilin (*FKBP5*) displayed a markedly greater interaction with the B variant (5.9 and 7.5 fold increase in comparison to the 2 other variants). These results were recapitulated by AP-western (**Supplementary. Fig. 29e**). We also found that different splice variants also exhibited preferential interactions with non-chaperone proteins. For example, the C variant specifically interacted with CRKL, an important scaffold in the receptor tyrosine kinase pathway, uncovering a potentially new link between GPCR and RTK signaling[3]. The specificity of the interaction with CRKL was validated by AP-western (**Supplementary. Fig. 29f**). Taken together, these GRK6 splice variant results indicate that AP-SWATH can effectively measure small modulations in protein interactions between splice variants using the approach presented here.

Supplementary references

1. Gurevich, E.V., Tesmer, J.J., Mushegian, A. & Gurevich, V.V. G protein-coupled receptor kinases: more than just kinases and not only for GPCRs. *Pharmacol Ther* **133**, 40-69 (2012).
2. Taipale, M. et al. Quantitative Analysis of Hsp90-Client Interactions Reveals Principles of Substrate Recognition. *Cell* **150**, 987-1001 (2012).
3. Pyne, N.J. & Pyne, S. Receptor tyrosine kinase-G-protein-coupled receptor signalling platforms: out of the shadow? *Trends Pharmacol Sci* **32**, 443-450 (2011).

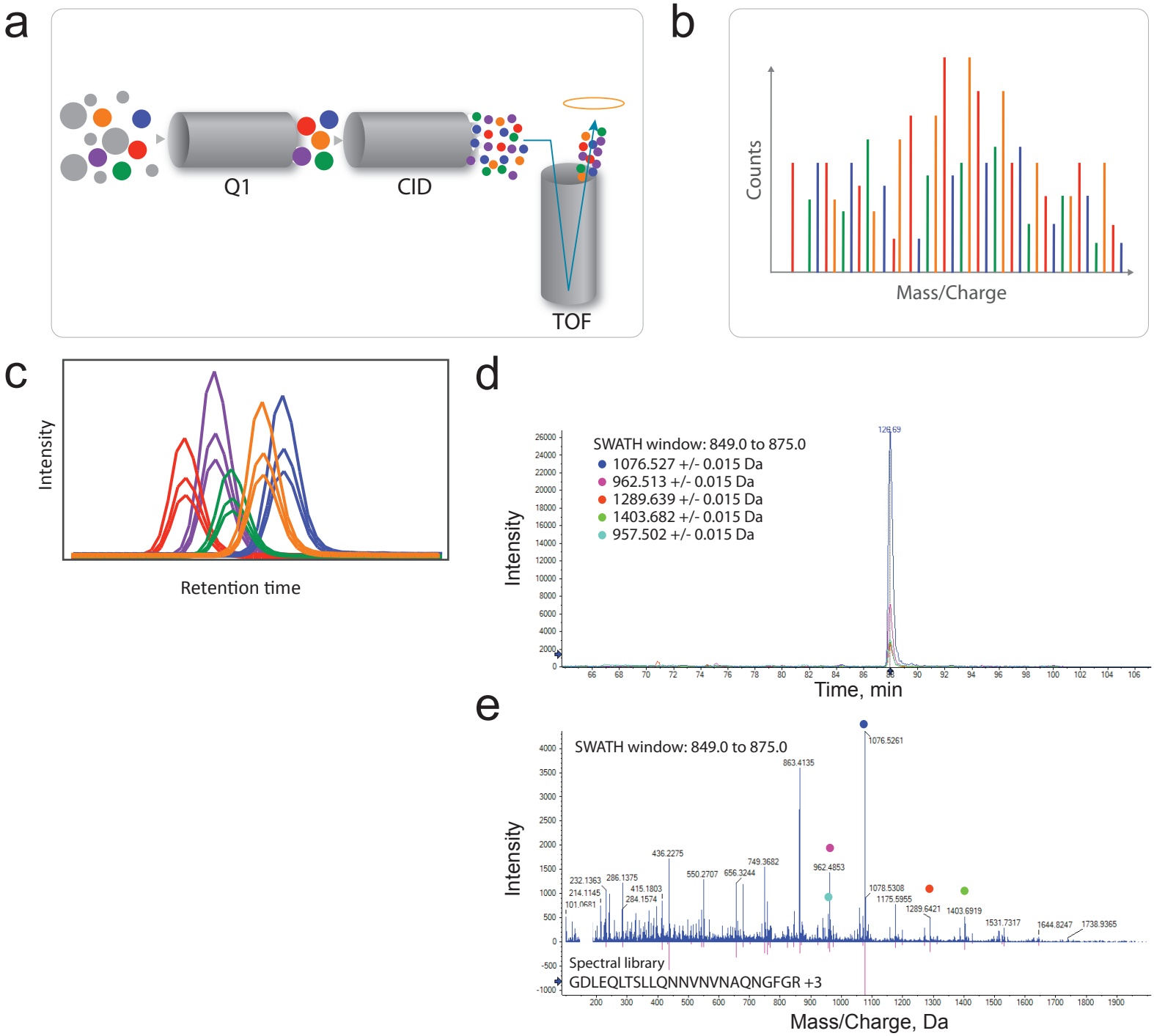

Supplementary Figure 1. Overview of the SWATH data acquisition process and data extraction. a) A TripleTOF(TM) 5600 was used in SWATH acquisition mode where a wide band isolation Q1 (25 amu) was used to transmit ions for fragmentation prior to detection by the TOF analyzer. b) Cartoon representation of a SWATH MS/MS spectrum showing peaks as detected from co-eluting and co-isolated species. c) By aligning extracted ion chromatograms for fragments for each peptide based on retention time, different clusters of MS/MS peaks are revealed. Similar to targeted mass spectrometry acquisition such as selected reaction monitoring (SRM), integration of the peak intensities for a given species can be used to calculate its relative abundance across samples. Identification of the species being quantified is based on a post-acquisition analysis: matching to a spectral library is employed here. Note that we depicted here the process for only one of the 25 amu swaths: however, the instrument in fact samples 32 x 25 amu swaths, covering the mass range 400-1250 amu with a cycle time of 3.25 seconds. d) Extracted ion chromatogram for a peptide in the PeakView SWATH plug-in. (e) Matches between the library spectrum (bottom) and SWATH (top) for the peptide shown in d.

a

Sample index	
1 - CDK4 WT BR1 TR1	15 - CDK4 R24C BR3 TR1
2 - CDK4 WT BR1 TR2	16 - CDK4 R24C BR3 TR2
3 - CDK4 WT BR1 TR2	17 - CDK4 R24C BR3 TR3
4 - CDK4 WT BR2 TR1	18 - CDK4 R24H BR1 TR1
5 - CDK4 WT BR2 TR2	19 - CDK4 R24H BR1 TR2
6 - CDK4 WT BR2 TR3	20 - CDK4 R24H BR1 TR2
7 - CDK4 WT BR3 TR1	21 - CDK4 R24H BR1 TR3
8 - CDK4 WT BR3 TR2	22 - CDK4 R24H BR2 TR1
9 - CDK4 WT BR3 TR3	23 - CDK4 R24H BR2 TR2
10 - CDK4 R24C BR1 TR1	24 - CDK4 R24H BR2 TR3
11 - CDK4 R24C BR1 TR2	25 - CDK4 R24H BR3 TR1
12 - CDK4 R24C BR1 TR3	26 - CDK4 R24H BR3 TR2
13 - CDK4 R24C BR2 TR2	27 - CDK4 R24H BR3 TR3
14 - CDK4 R24C BR2 TR3	

b

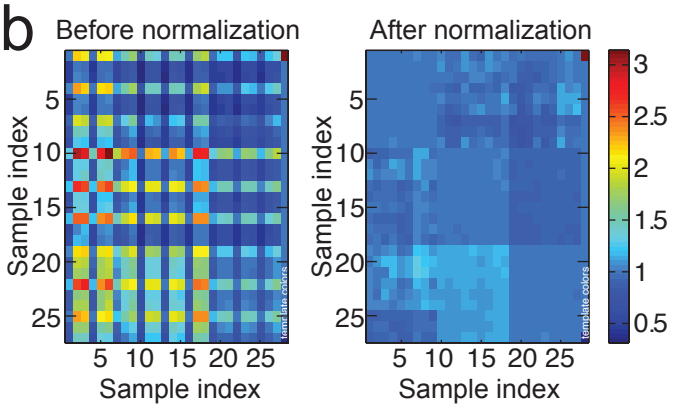

c

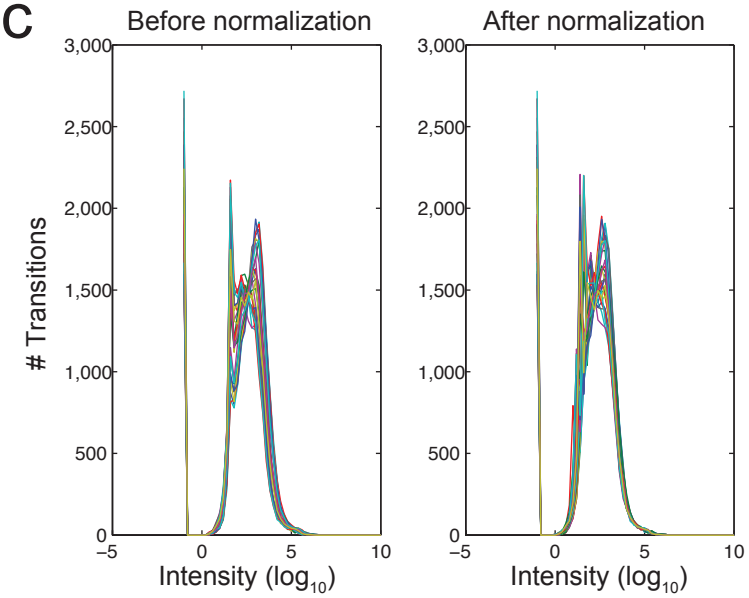

d

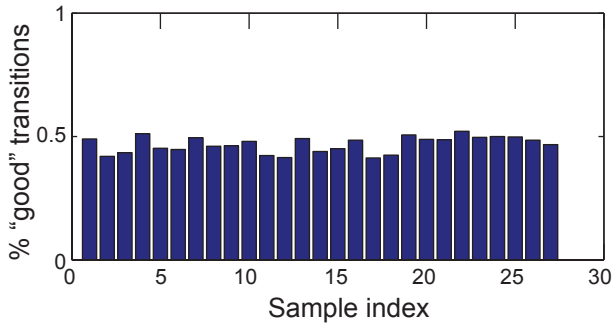

Supplementary Figure 2. Normalization of the transitions for the large dataset (9 replicates each CDK4 WT, R24C, R24H; Supplementary Table 2; group 5). a) Sample index; BR = biological replicate; TR = technical replicate. b) Most likely area ratios between samples before and after normalization. c) Intensity histograms before and after normalization (the different lines point to different samples). d) Percentage of transitions which exceed the measurement reproducibility filter (see Methods for details).

a

Sample index	
1 - GFP control BR1	7 - MEPCE BR1
2 - GFP control BR2	8 - MEPCE BR2
3 - GFP control BR3	9 - MEPCE BR3
4 - EIF4A2 BR1	
5 - EIF4A2 BR2	
6 - EIF4A2 BR3	

b

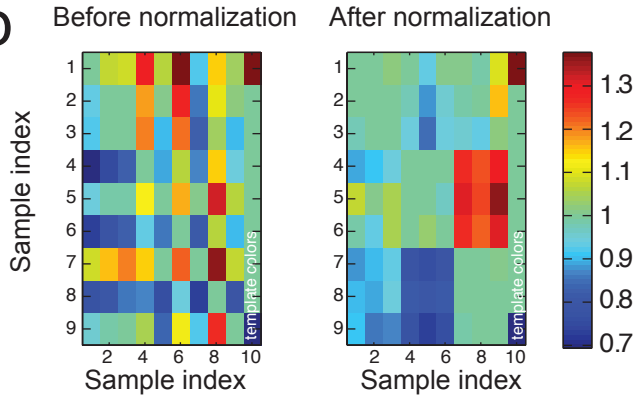

c

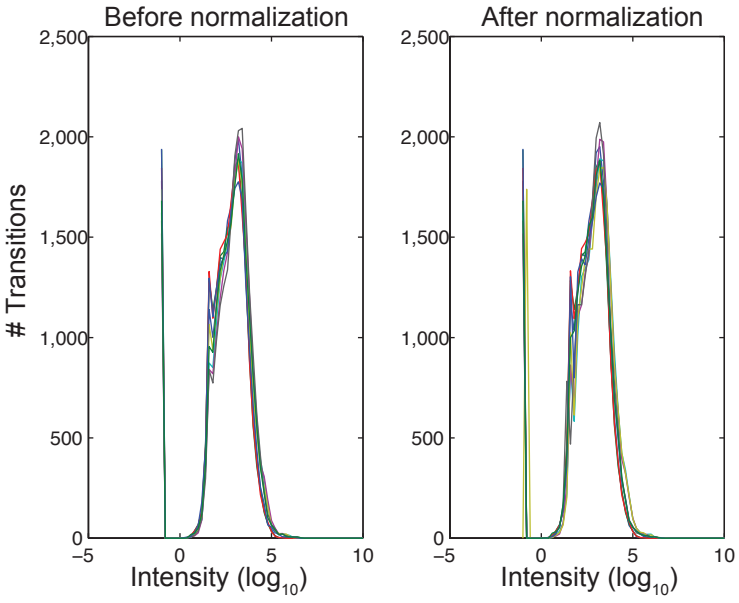

d

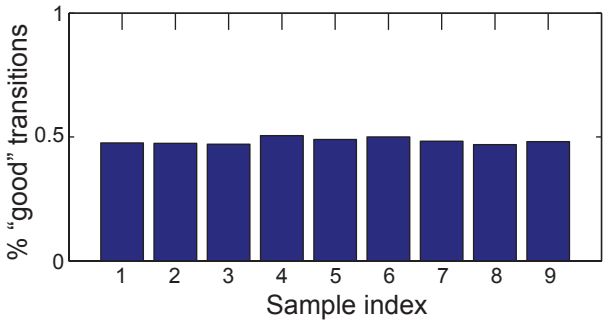

Supplementary Figure 3. Normalization of the transitions for EIF4A2/MEPCE dataset (group 6). a) Sample index; BR = biological replicate. b) Most likely area ratios between samples before and after normalization. c) Intensity histograms before and after normalization (the different lines point to different samples). d) Percentage of transitions which exceed the measurement reproducibility filter (see Methods for details).

a

Sample index
1 - empty control - DMSO - BR1
2 - empty control - DMSO - BR2
3 - CDK4 WT - DMSO - BR1
4 - CDK4 WT - DMSO - BR2
5 - CDK4 R24C - DMSO - BR1
6 - CDK4 R24C - DMSO - BR2
7 - CDK4 R24H - DMSO - BR1
8 - CDK4 R24H - DMSO - BR2

b

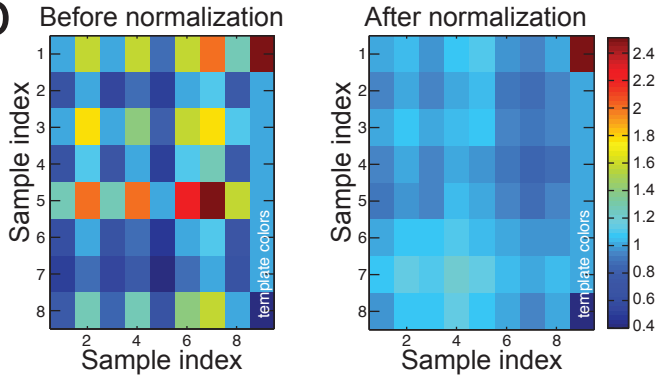

c

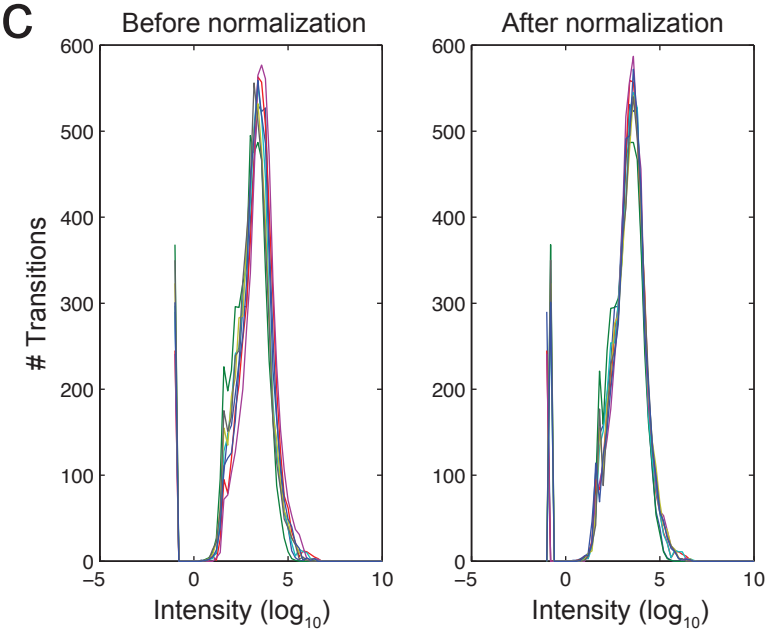

d

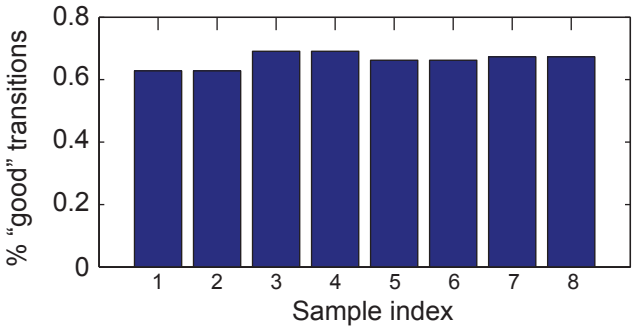

Supplementary Figure 4A. Normalization of the transitions for the DMSO treated CDK4 dataset with controls (group 3). a) Sample index; BR = biological replicate. b) Most likely area ratios between samples before and after normalization. c) Intensity histograms before and after normalization (the different lines point to different samples). d) Percentage of transitions which exceed the measurement reproducibility filter (see Methods for details).

a

Sample index
1 - empty control - NVP - BR1
2 - empty control - NVP - BR2
3 - CDK4 WT - NVP - BR1
4 - CDK4 WT - NVP - BR2
5 - CDK4 R24C - NVP - BR1
6 - CDK4 R24C - NVP - BR2
7 - CDK4 R24H - NVP - BR1
8 - CDK4 R24H - NVP - BR2

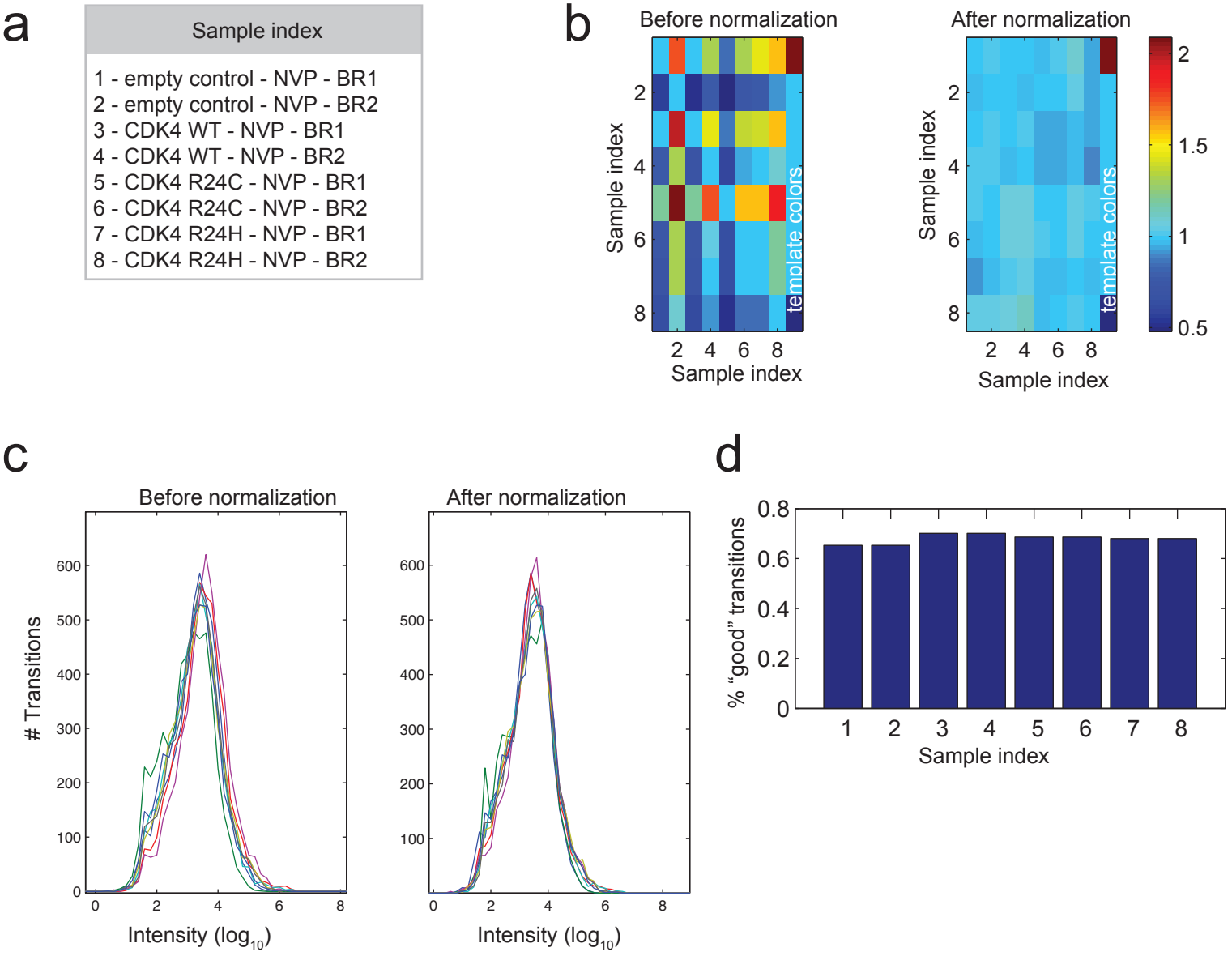

Supplementary Figure 4B. Normalization of the transitions for the NVP-AUY922 treated CDK4 dataset with controls (group 3). a) Sample index; BR = biological replicate. b) Most likely area ratios between samples before and after normalization. c) Intensity histograms before and after normalization (the different lines point to different samples). d) Percentage of transitions which exceed the measurement reproducibility filter (see Methods for details).

a

Sample index	
1 - CDK4 WT BR1	7 - CDK4 R24H BR1
2 - CDK4 WT BR2	8 - CDK4 R24H BR2
3 - CDK4 N41S BR1	9 - CDK4 S52N BR1
4 - CDK4 N41S BR2	10- CDK4 S52N BR2
5 - CDK4 R24C BR1	
6 - CDK4 R24C BR2	

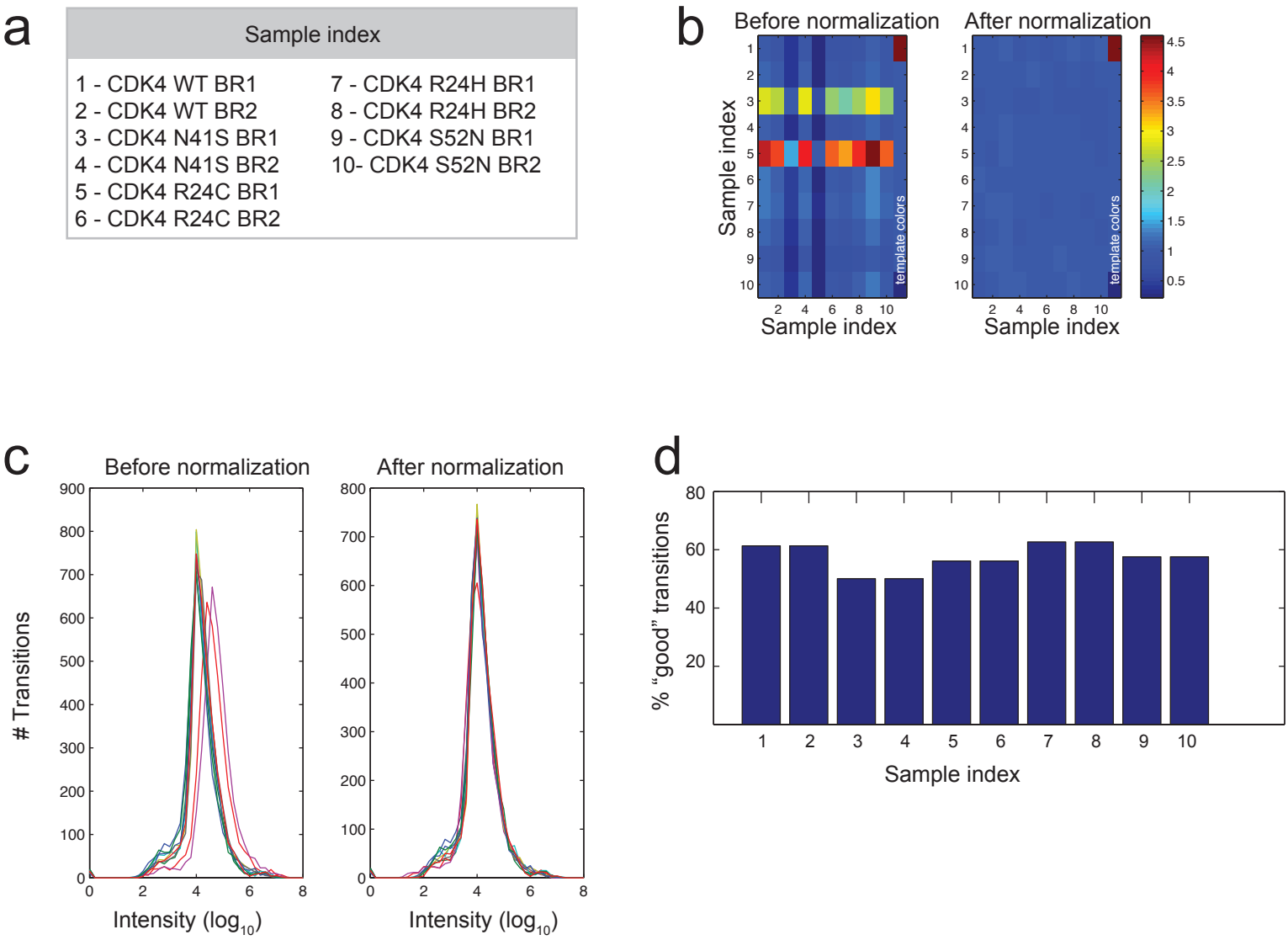

Supplementary Figure 5. Normalization of the transitions for the extended set of CDK4 mutant analysis (group 2). a) Sample index; BR = biological replicate. b) Most likely area ratios between samples before and after normalization. c) Intensity histograms before and after normalization (the different lines point to different samples). d) Percentage of transitions which exceed the measurement reproducibility filter (see Methods for details).

a

Sample index	
1 - GRK6B BR2	7 - GRK6A BR4
2 - GRK6B BR3	8 - GRK6A BR5
3 - GRK6B BR4	9 - GRK6C BR2
4 - GRK6B BR5	10 - GRK6C BR3
5 - GRK6A BR2	11 - GRK6C BR4
6 - GRK6A BR3	12 - GRK6C BR5

b

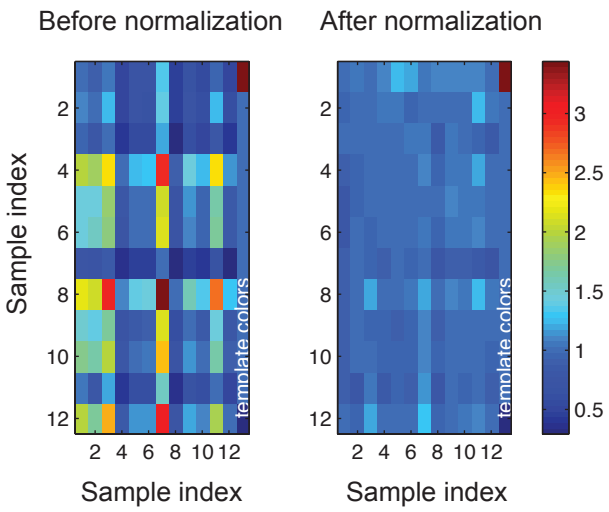

c

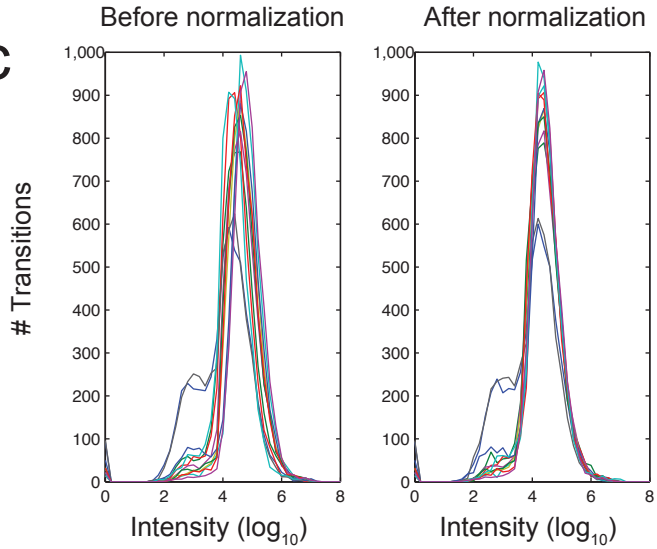

d

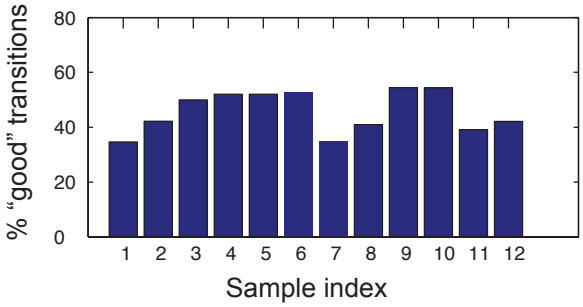

Supplementary Figure 6. Normalization of the transitions for the GRK6 splice variant samples (group 4). a) Sample index; BR = biological replicate. b) Most likely area ratios between samples before and after normalization. c) Intensity histograms before and after normalization (the different lines point to different samples). d) Percentage of transitions which exceed the measurement reproducibility filter (see Methods for details).

a

Sample index	
1 - CDK4 WT BR1	7 - CDK4 R24H BR1
2 - CDK4 WT BR2	8 - CDK4 R24H BR2
3 - CDK4 WT BR3	9 - CDK4 R24H BR3
4 - CDK4 R24C BR1	
5 - CDK4 R24C BR2	
6 - CDK4 R24C BR3	

b

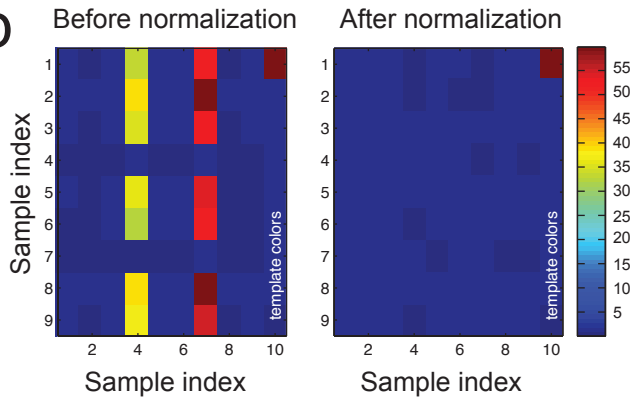

c

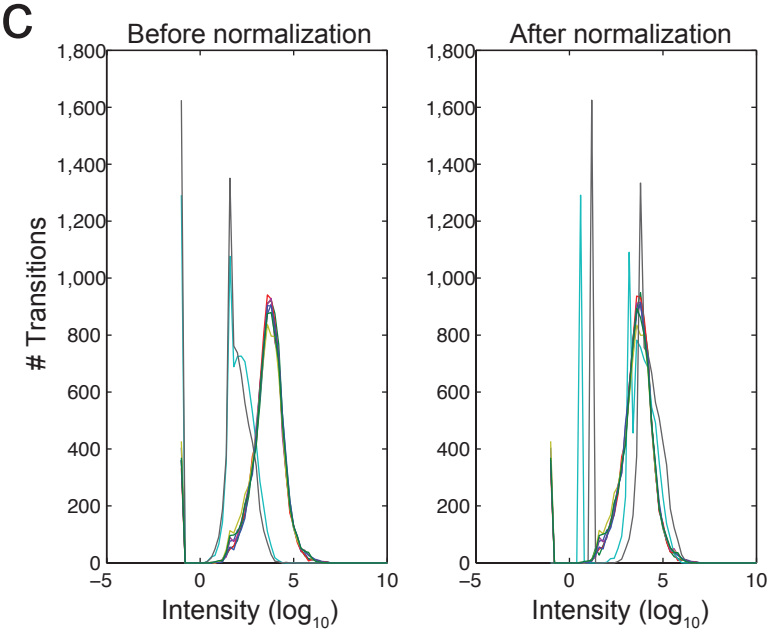

d

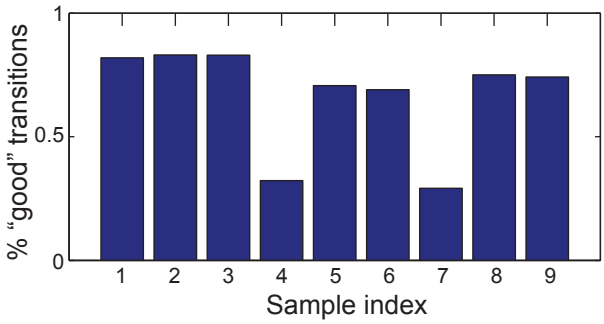

Supplementary Figure 7. Normalization of the transitions for the CDK4 dataset from 2011 (group 1). a) Sample index; BR = biological replicate. b) Most likely area ratios between samples before and after normalization. c) Intensity histograms before and after normalization (the different lines point to different samples). d) Percentage of transitions which exceed the measurement reproducibility filter (see Methods for details). Note the overall lower quality (due to the overall lower intensiy) of samples 4 and 7.

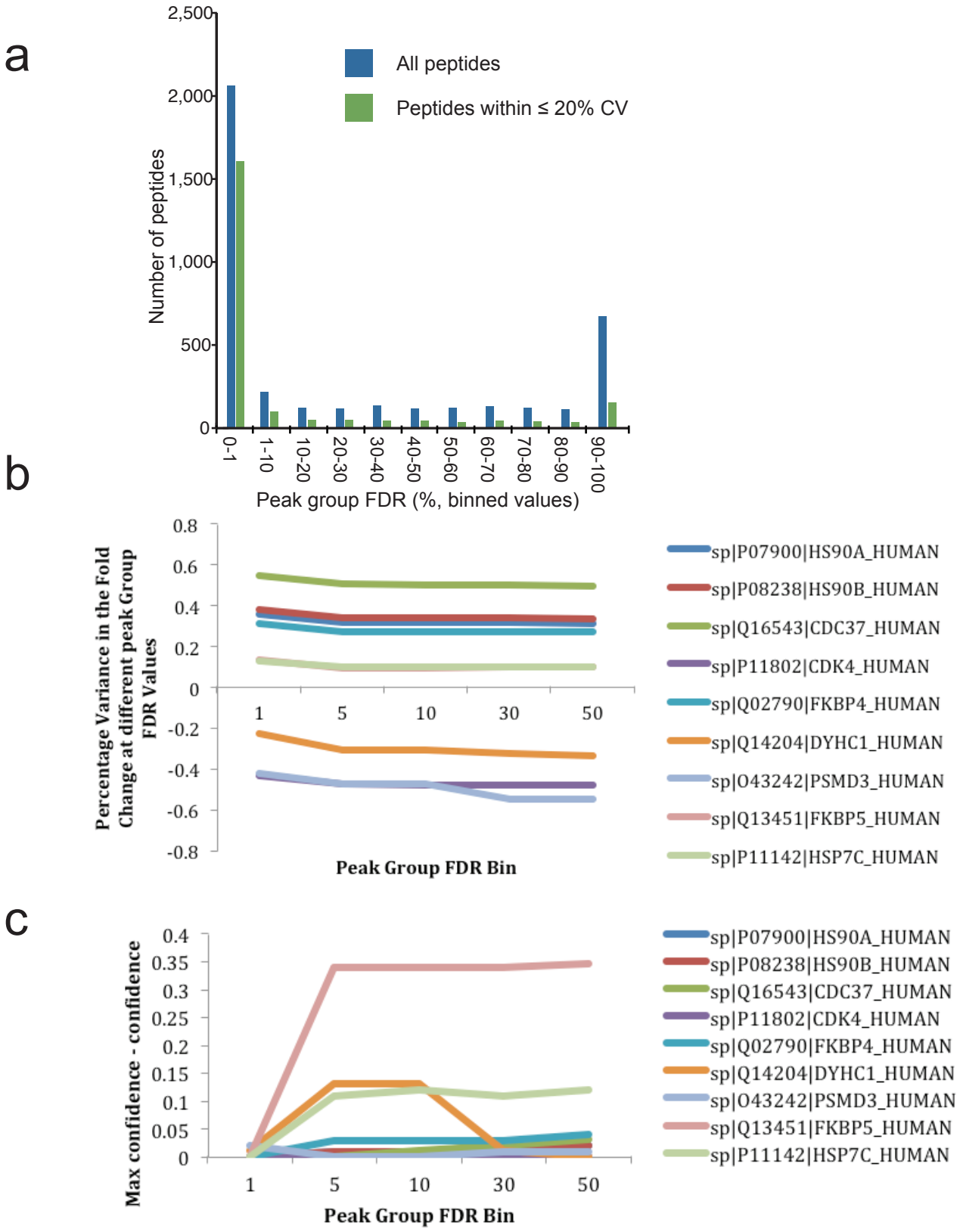

Supplementary Figure 8. Effect of the peak group FDR on measurement reproducibility and Fold Change calculation. a) From the CDK4 WT samples (n = 9; group 5), the number of peptides extracted at the indicated FDR bins is plotted alongside the number of those peptides which have a reproducibility ≤ 20% CV. b) Impact of different extraction FDR cutoffs on the value of the fold change for selected CDK4 associated proteins. c) Impact of different extraction FDR cutoffs on the confidence (plotted as a difference to the maximal confidence detected with the 1% FDR cutoff) of the Fold Change.

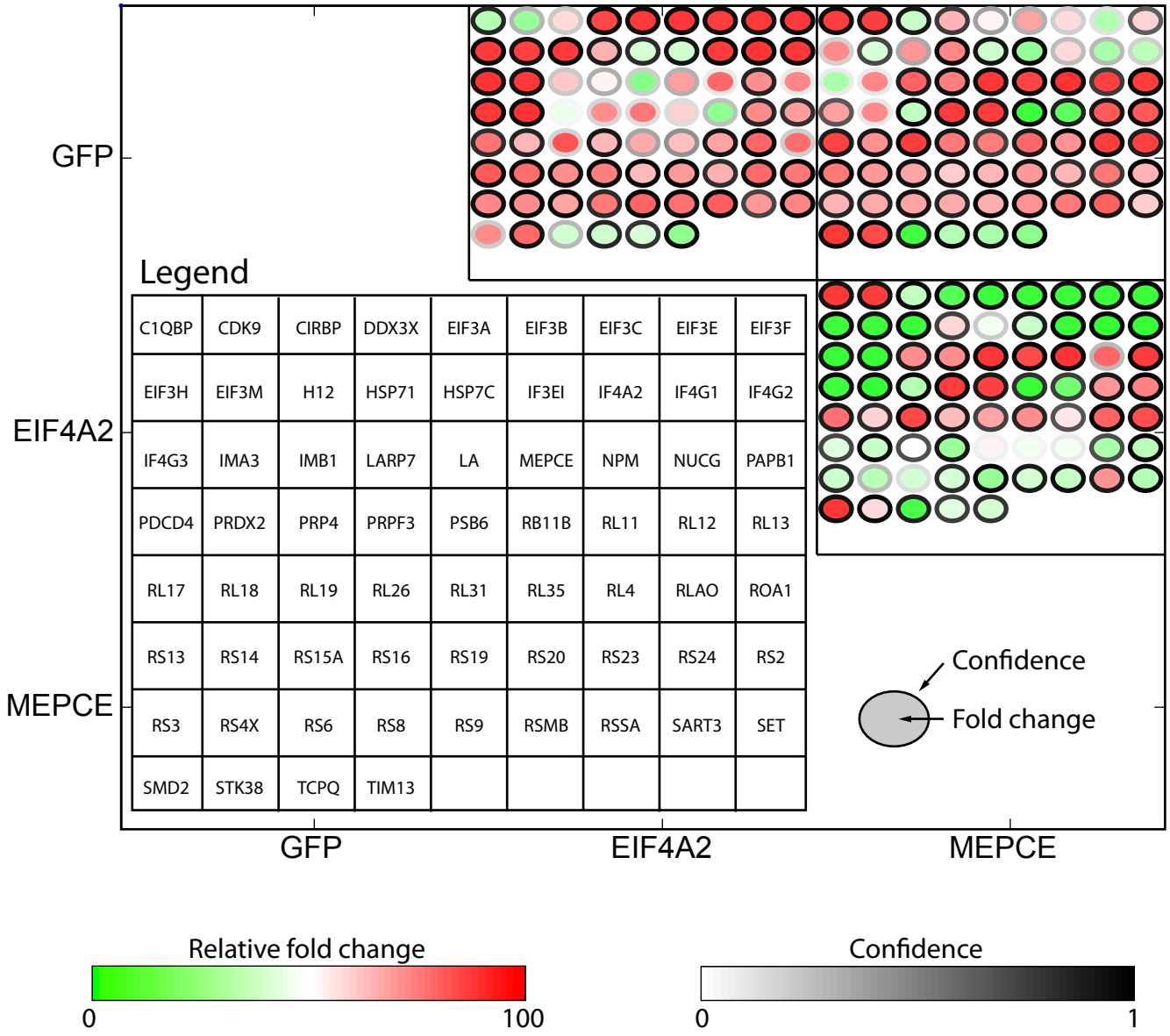

Supplementary Figure 9: Global view of MEPCE and EIF4A2 dataset shown in Figs 2a and b (group 6). Pairwise comparisons for the entire dataset. Only data for proteins with a Fold Change confidence ≥ 0.75 (and that have passed the other filters as described in Methods) in at least one pairwise comparison are displayed. The proteins are arranged in the matrix by alphabetical order (across the entire dataset) in the same order for all comparisons (see legend). Relative Fold Change values are displayed by the inside color of the circles (green to red scale). Confidence values are shown by the grey shading of the circle outline. Protein names are as per Uniprot; See Supplementary Table 1 for Official Gene Symbols and aliases.

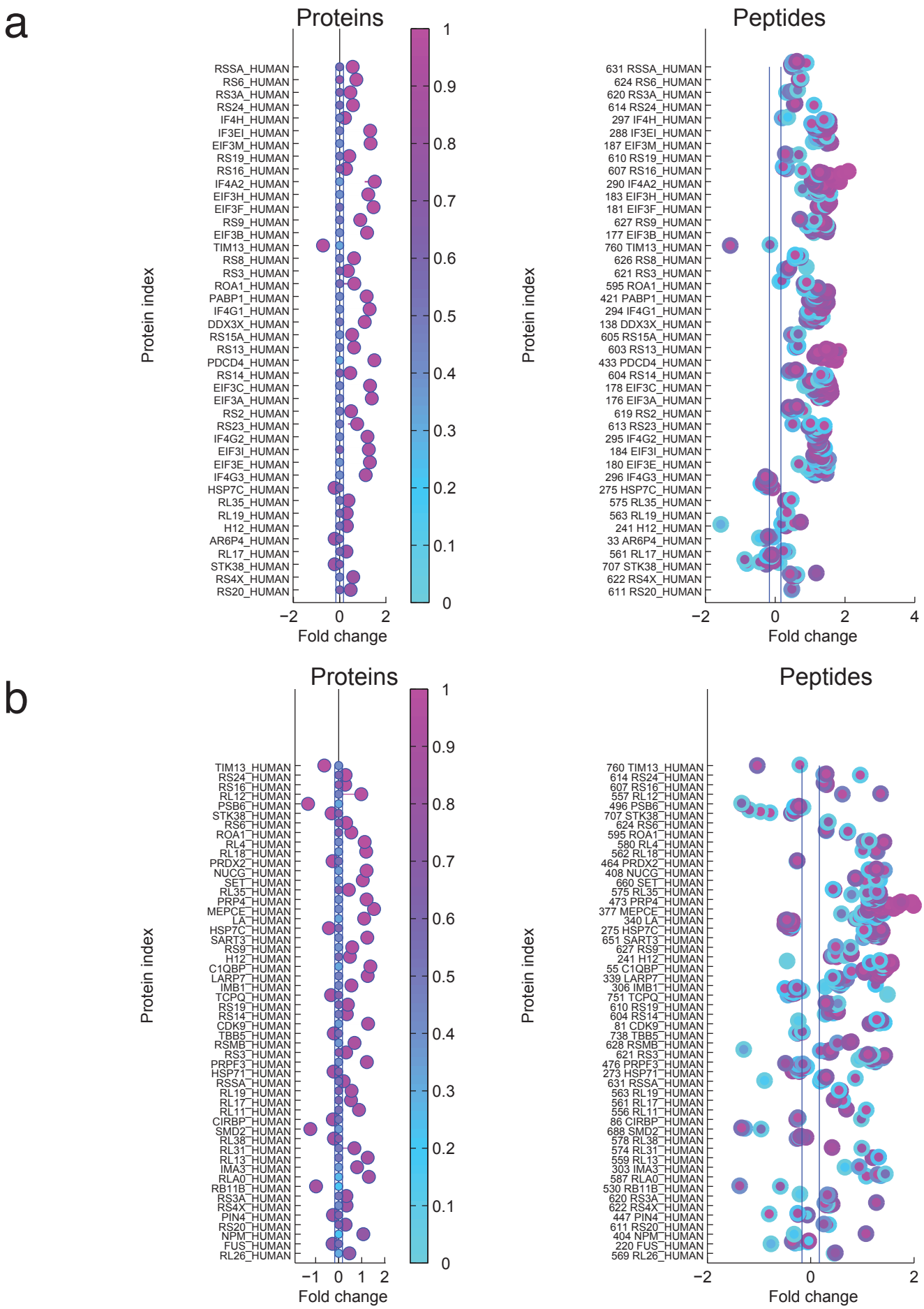

Supplementary Figure 10. Fold Changes and confidence scores for the comparison of EIF4A2 (a) and MEPCE (b) to GFP control (group 6). *Left panels*; protein Fold Change values where confidence is ≥ 0.75. *Right panels*; peptide level Fold Change with the confidence represented by the main colour and the signal-to-noise score by the outline colour. Labels are Uniprot protein names; see Supplementary Table 1 for Official Gene Symbols.

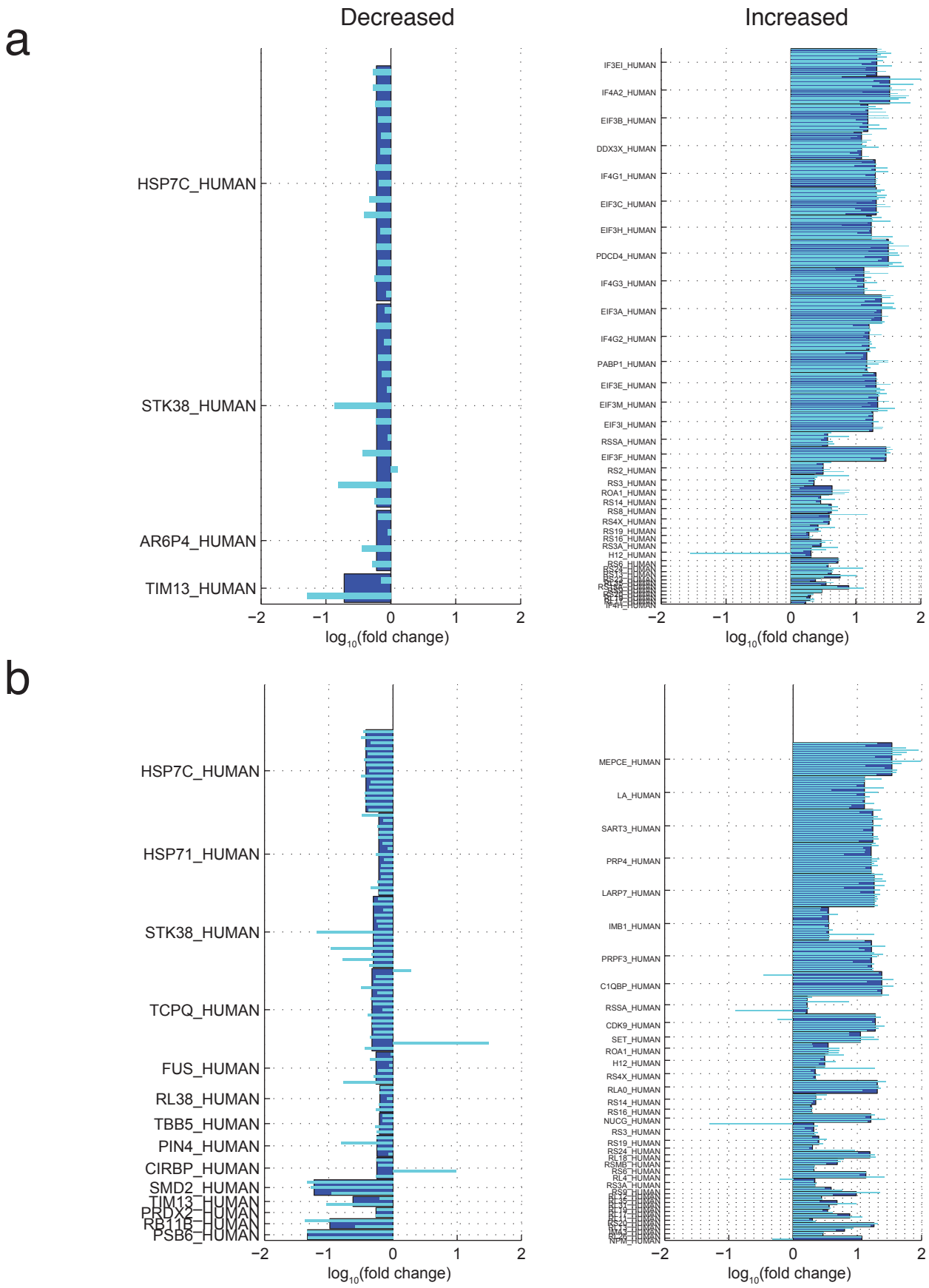

Supplementary Figure 11. Histogram representation of protein and peptide fold change of the EIF4A2 (a) and MEPCE (b) samples in comparison to a GFP negative control (group 6). *Left panel*; protein level and peptide level Fold Change for proteins identified with a confidence Fold Change ≥ 0.75 to be decreased in MEPCE or EIF4A2 in comparison to a negative GFP control. *Right panel*; high confidence upregulated proteins. Labels are Uniprot protein names. The dark blue boxes are the protein fold changes, and the light blue are the peptides used for Fold Change calculation.

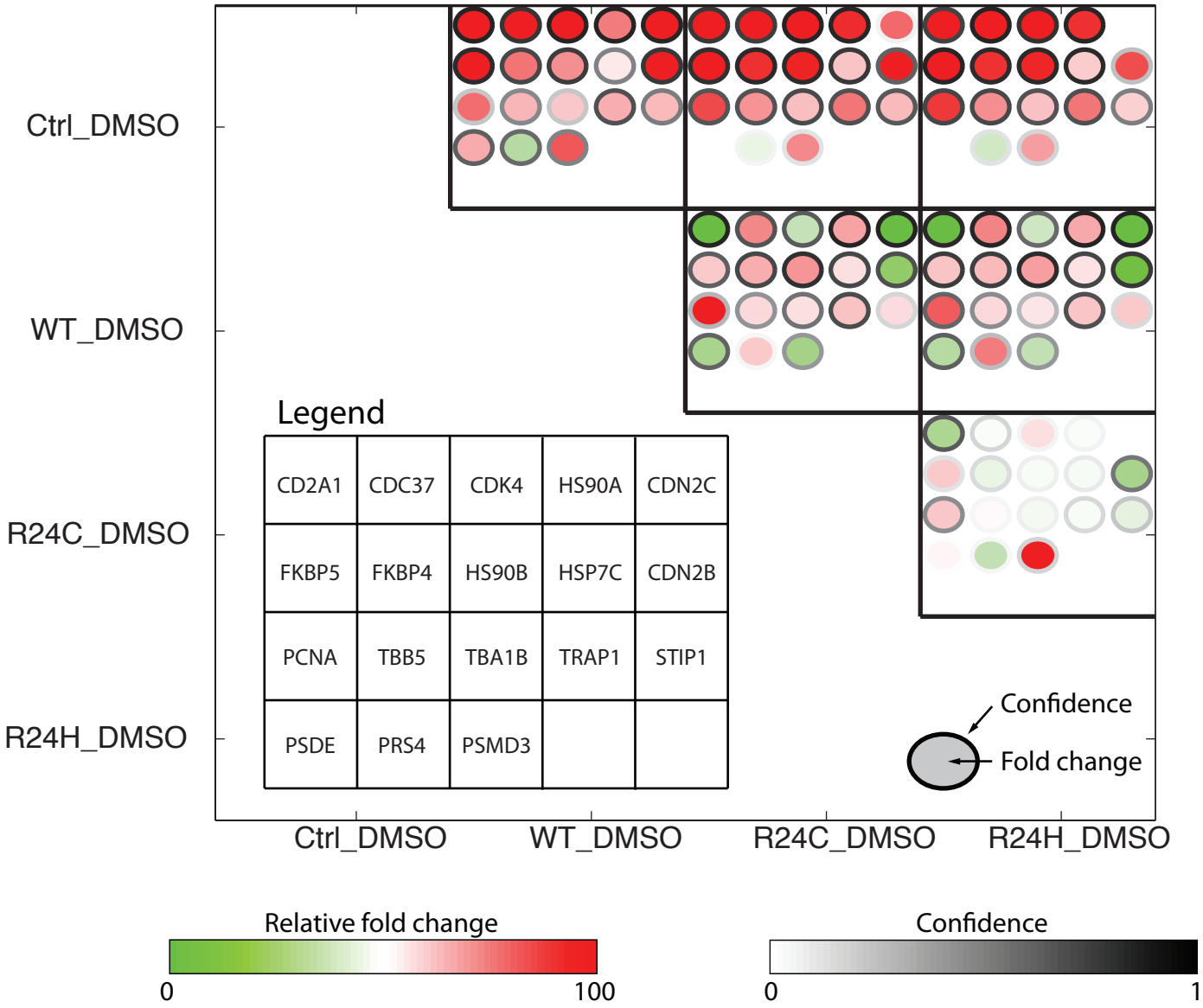

Supplementary Figure 12. Global view of mock-treated CDK4 dataset shown in Fig. 4b; comparison to FLAG negative control (group 3). Pairwise comparisons for the entire dataset. Only data for proteins with a Fold Change confidence ≥ 0.75 (and that have passed the other filters as described in Methods) in at least one pairwise comparison are displayed. The proteins are arranged by decreasing confidence (across the entire dataset) in the same order for all comparisons (see legend). Relative Fold Change values are displayed by the inside color of the circles (green to red scale). Confidence values are shown by the grey shading of the circle outline. Protein names are as per Uniprot; See Supplementary Table 1 for Official Gene Symbols and aliases.

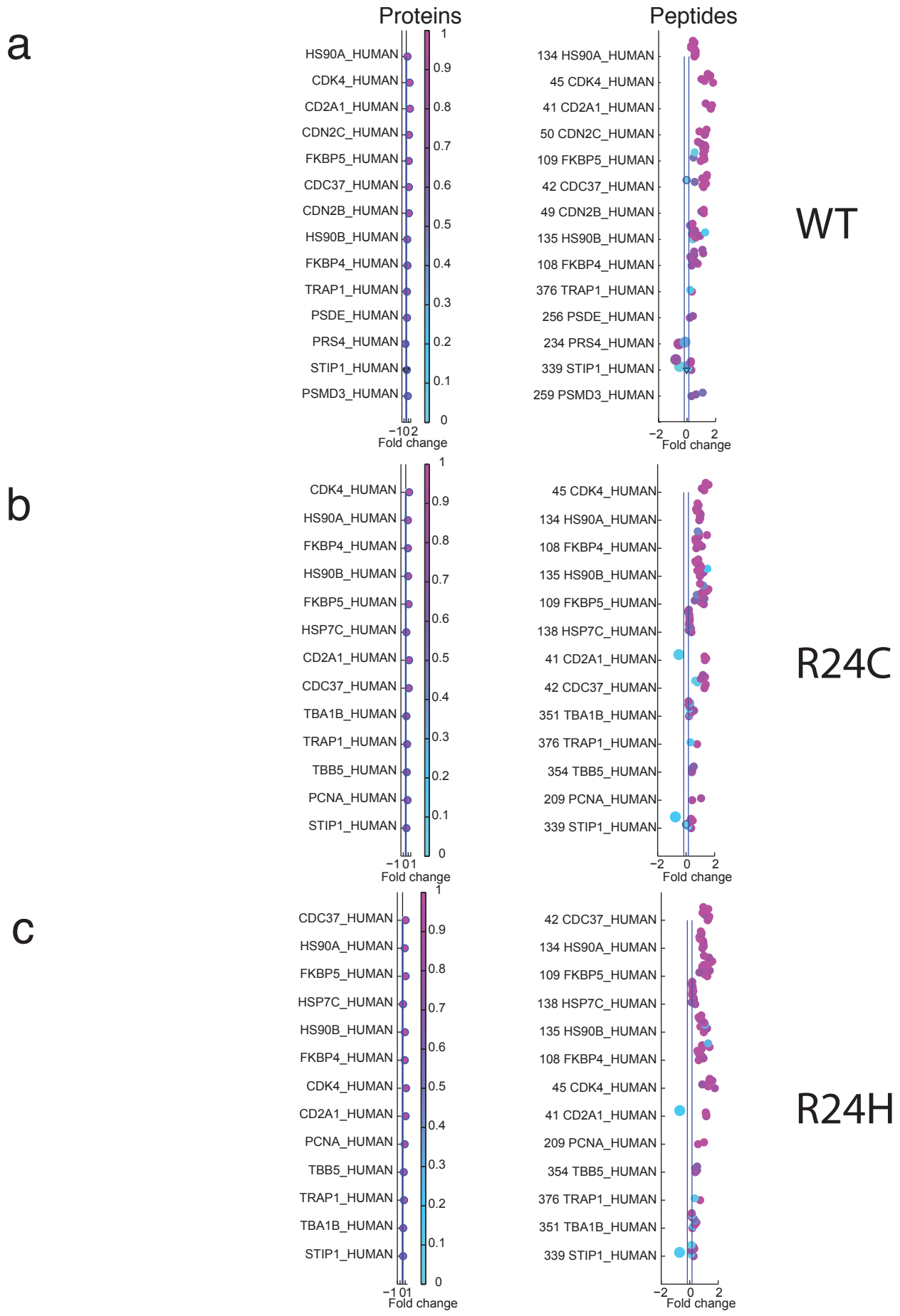

Supplementary Figure 13. Fold Changes and confidence scores for comparison of CDK4 proteins to FLAG alone negative control (group 3). *Left panels*; protein Fold Change values where confidence is ≥ 0.75. *Right panels*; peptide level Fold Change with the confidence represented by the main colour and the signal-to-noise score by the outline colour. Labels are Uniprot protein names; see Supplementary Table 1 for Official Gene Symbols.

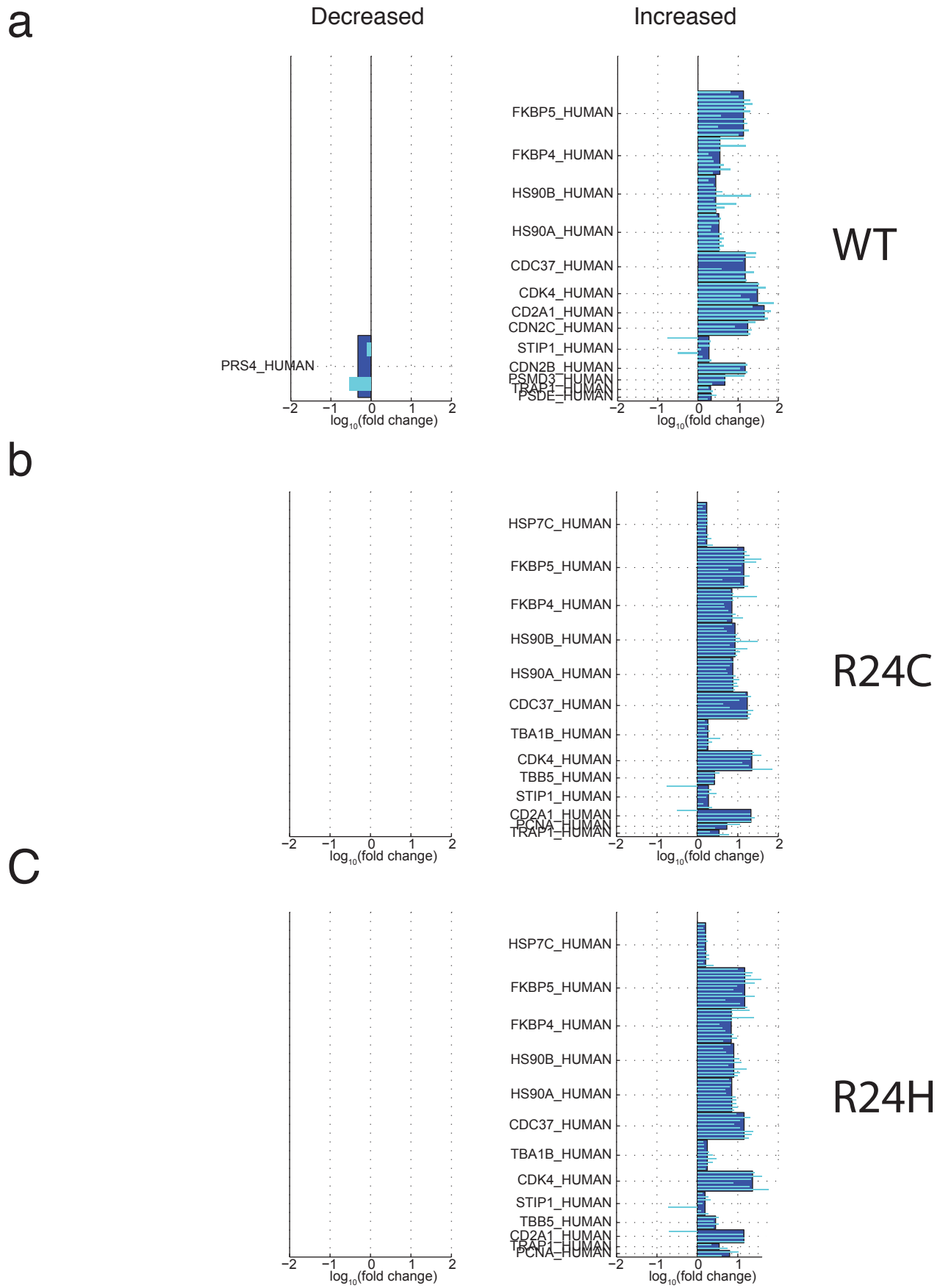

Supplementary Figure 14. Histogram representation of protein and peptide fold change of the CDK4 samples in comparison to a FLAG alone negative control (group 3). *Left panel*; protein level and peptide level Fold Change for proteins identified with a confidence Fold Change ≥ 0.75 to be decreased in the CDK4 in comparison to the negative control (FLAG alone). *Right panel*; high confidence upregulated proteins. Labels are Uniprot protein names. The dark blue boxes are the protein Fold Changes, and the light blue are the peptides used for Fold Change calculation.

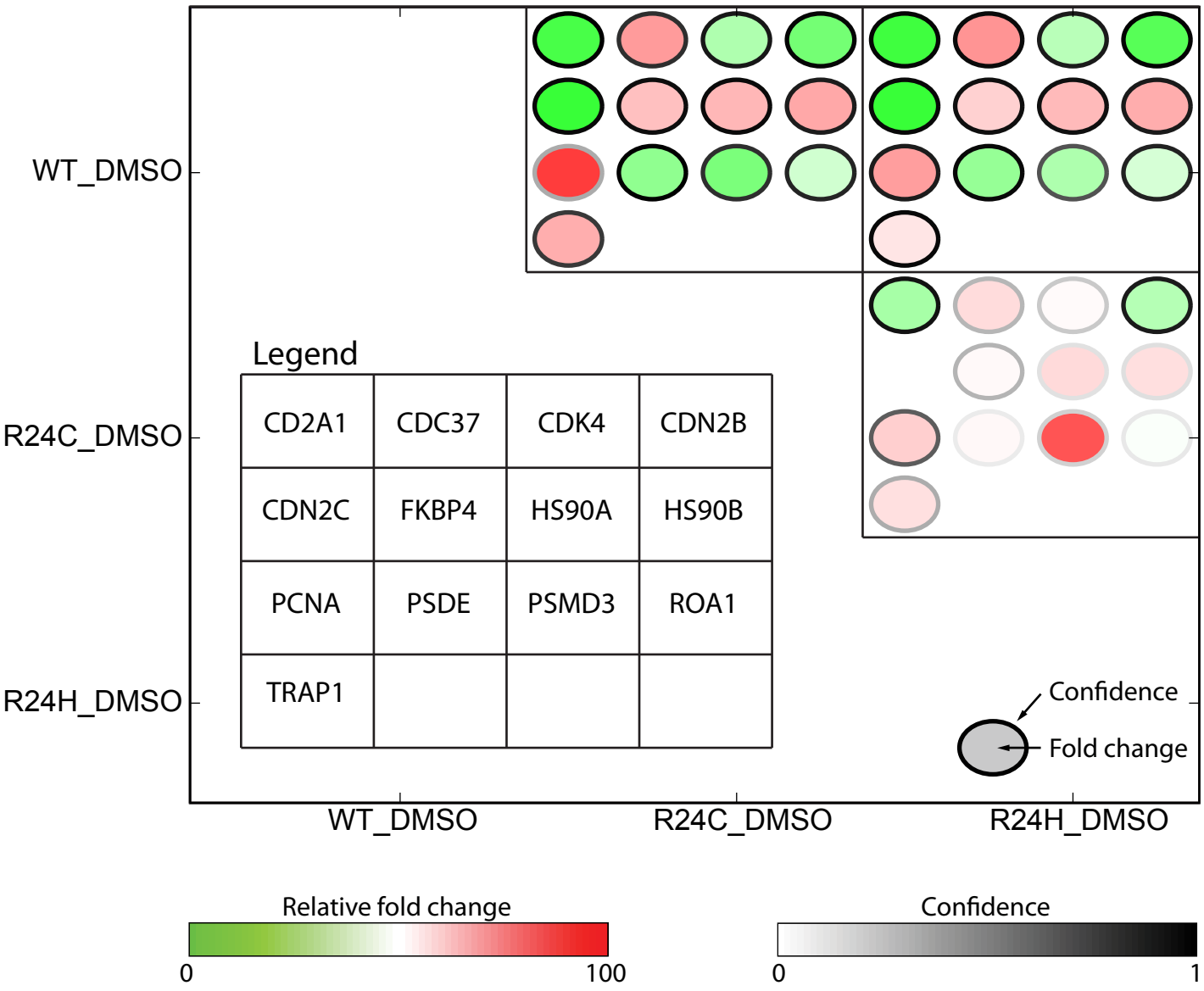

Supplementary Figure 15. Global view of mock treated CDK4 dataset shown in Fig. 4d; comparison of the mutants to CDK4 WT (group 3). Pairwise comparisons for the entire dataset. Only data for proteins with a Fold Change confidence ≥ 0.75 (and that have passed the other filters as described in Methods) in at least one pair-wise comparison are displayed. The proteins are arranged by decreasing confidence (across the entire dataset) in the same order for all comparisons (see legend). Relative Fold Change values are displayed by the inside color of the circles (green to red scale). Confidence values are shown by the grey shading of the circle outline. Protein names are as per Uniprot; See Supplementary Table 1 for Official Gene Symbols and aliases.

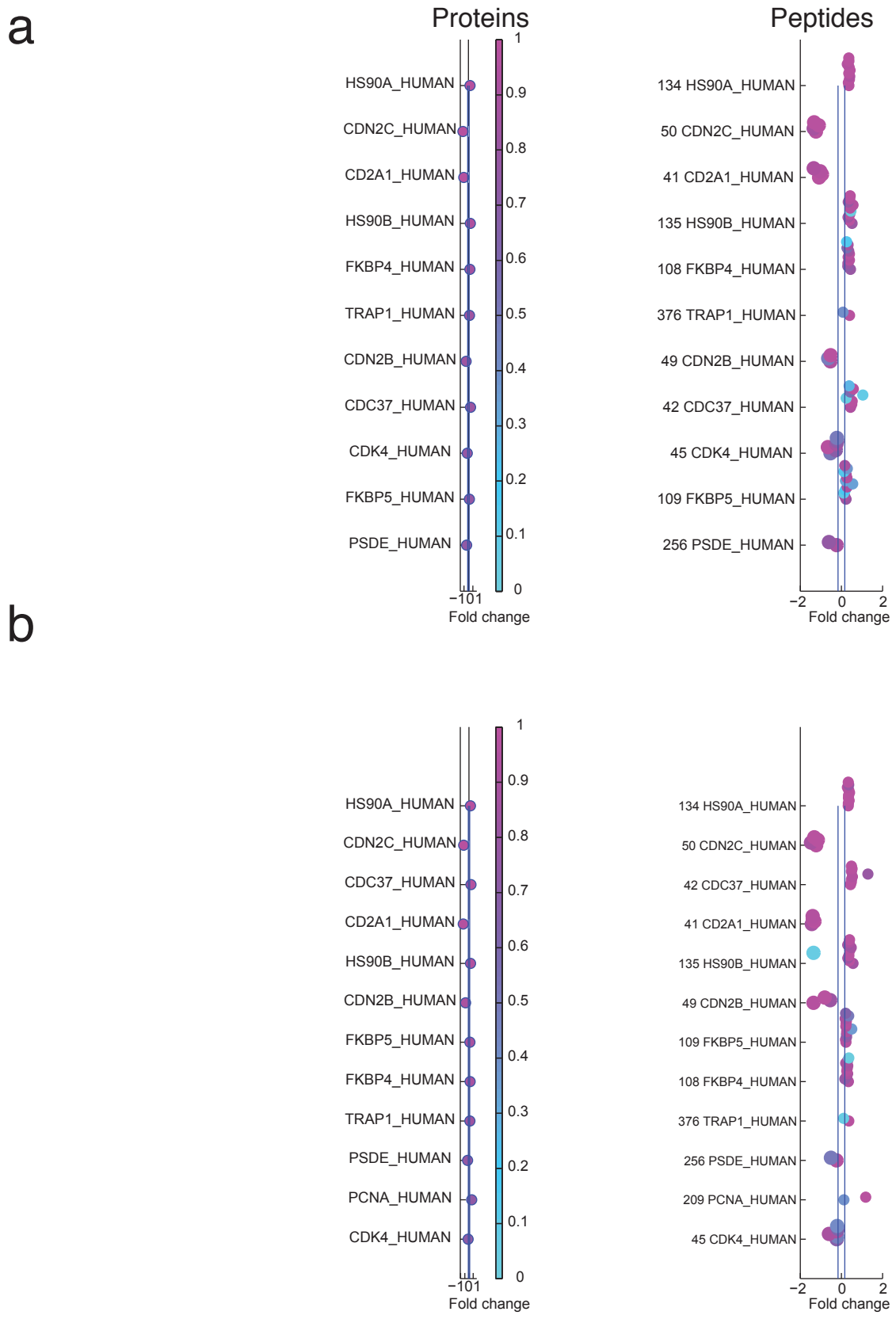

Supplementary Figure 16. Fold Change and confidence scores for the comparison of the CDK4 mutants (R24C (a) and R24H (b)) to CDK4 WT (group 3). *Left panels*; protein Fold Change values where confidence is ≥ 0.75. *Right panels*; peptide level Fold Change with the confidence represented by the main colour and the signal-to-noise score by the outline colour. Labels are Uniprot protein names; see Supplementary Table 1 for Official Gene Symbols.

a

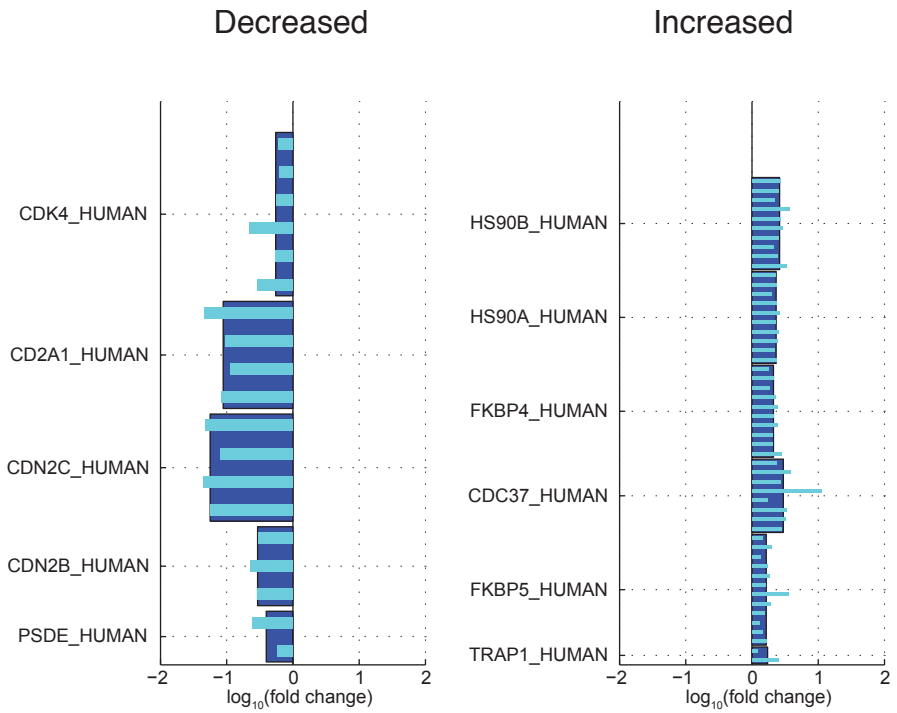

b

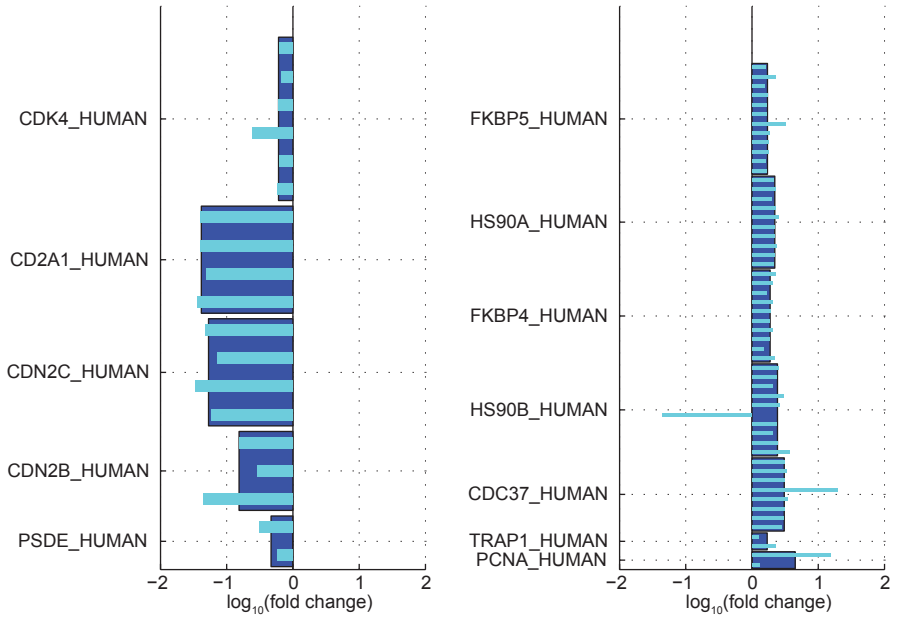

Supplementary Figure 17. Histogram representation of protein and peptide Fold Change of mock treated CDK4 mutants (R24C (a) and R24H (b)) as compared to CDK4 WT (group 3). *Left panel*; protein level and peptide level Fold Change for proteins identified with a confidence Fold Change ≥ 0.75 to be decreased in the mutants in comparison to the WT CDK4. *Right panel*; high confidence upregulated proteins. Labels are Uniprot protein names. The dark blue boxes are the protein Fold Changes, and the light blue are the peptides used for Fold Change calculation.

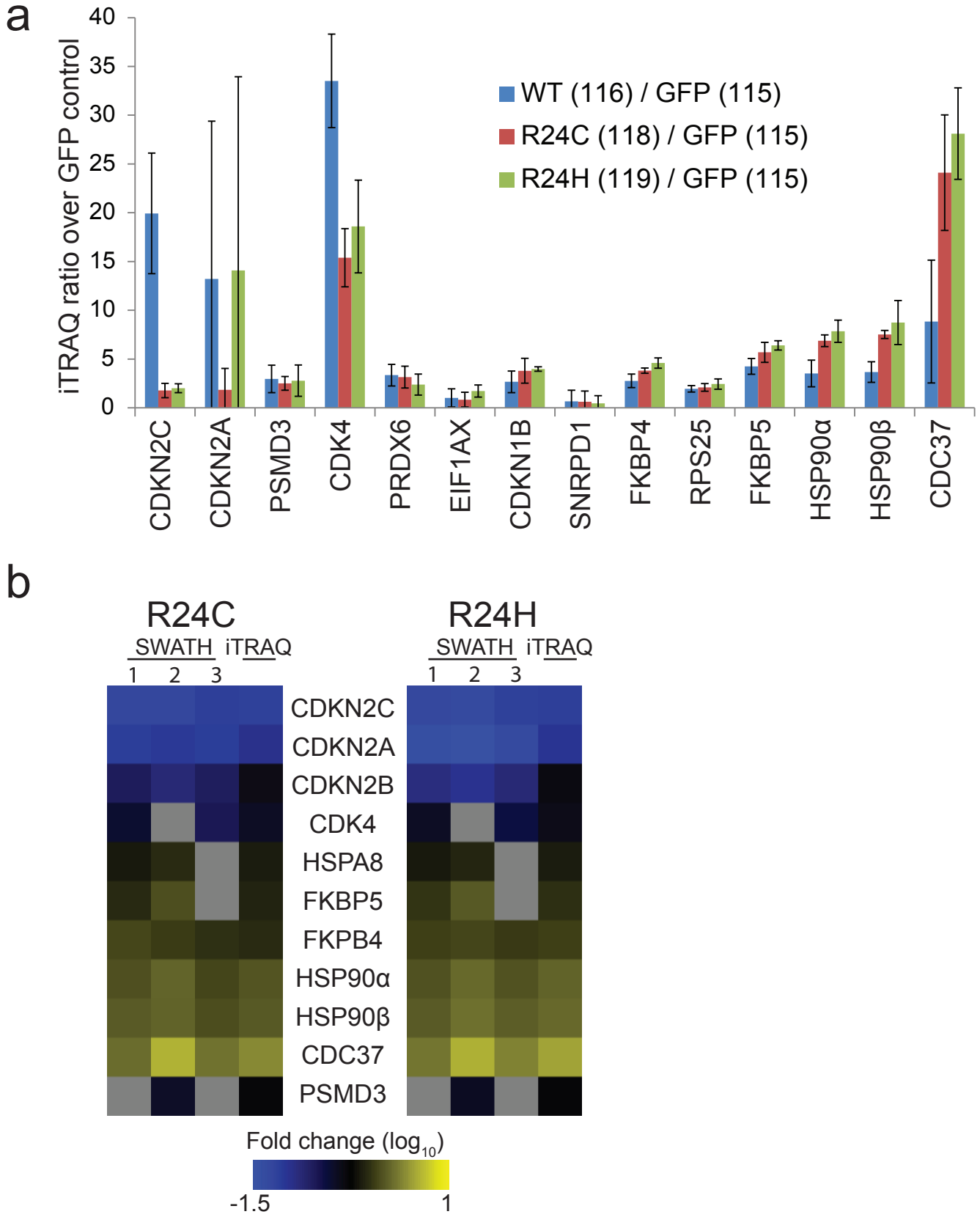

Supplementary Figure 18. Extended view of the iTRAQ dataset and comparison of iTRAQ ratios to the Fold Change across three SWATH dataset acquired over the course of 2 years (group 1, 3 and 5). a) Bar graph of average iTRAQ ratio from three biological replicate (empty FLAG control = 115; CDK4 WT = 116; CDK4 R24C = 118; CDK4 R24H = 119) and their standard deviation. Note that some large errors (e.g. CDKN2A) are due to the stochastic nature of iTRAQ where a particular protein was undetected in a given biological replicate. b) Heat map showing an extended comparison between SWATH and iTRAQ presented in Fig 4d. dataset #1 = group 1; dataset #2 = group 3; dataset #3 = group 5). The different SWATH datasets were acquired over 2 years.

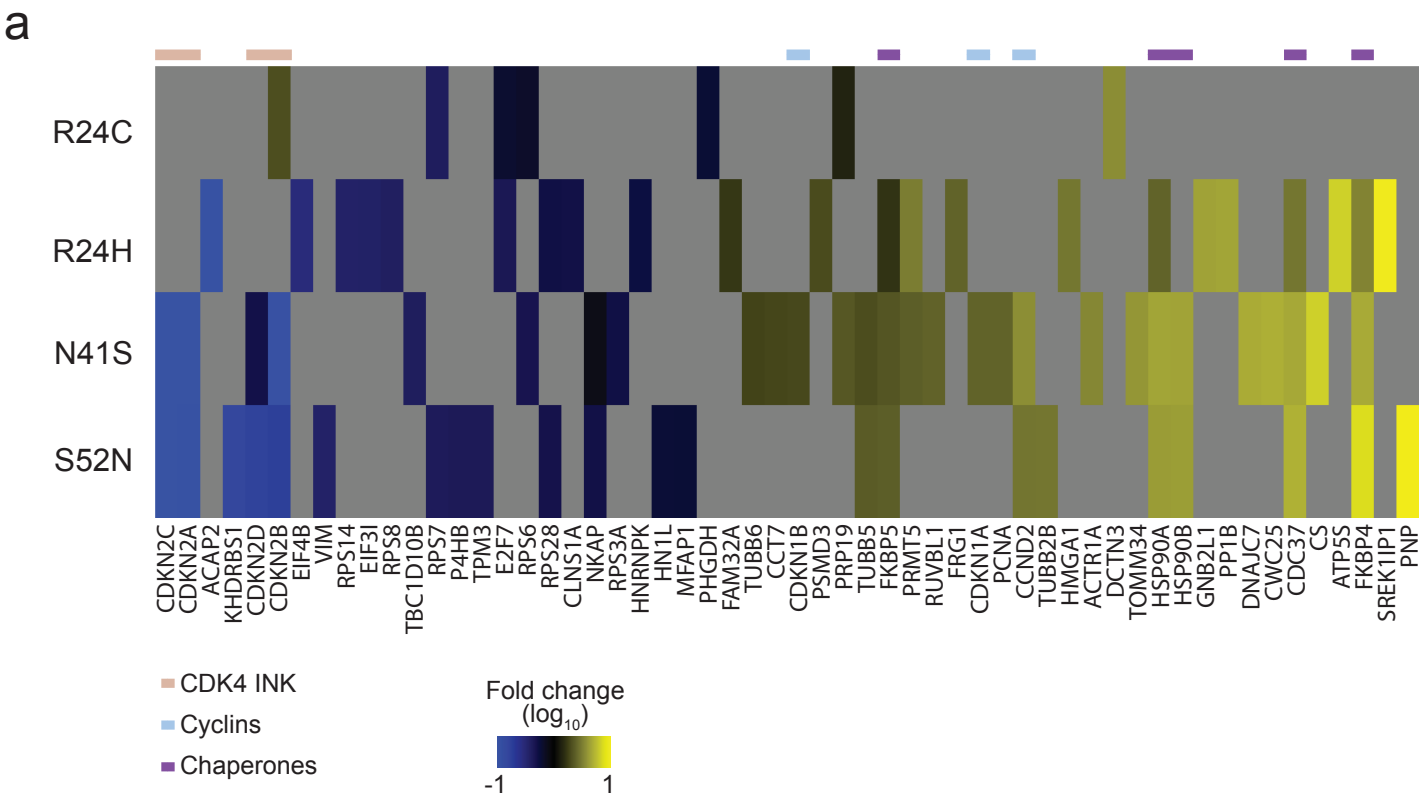

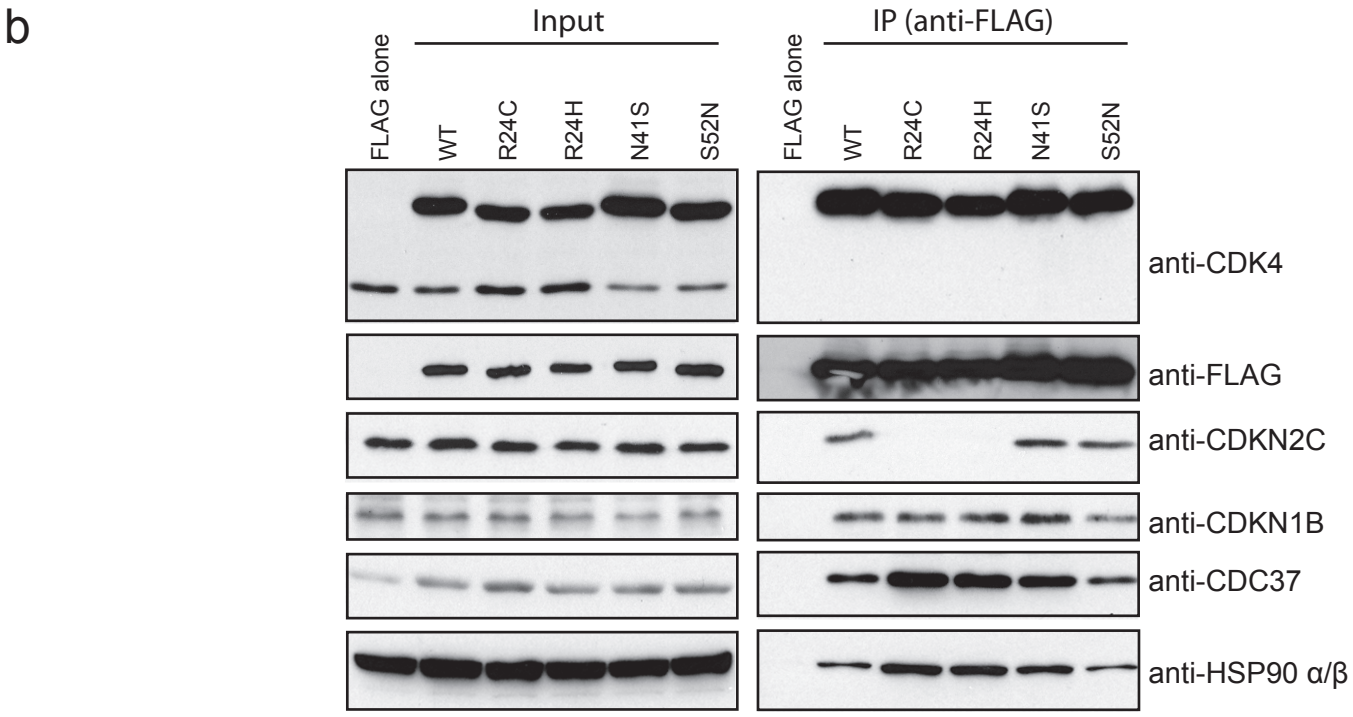

Supplementary Figure 19. Analysis of an expanded set of CDK4 mutants. a) heatmap of the data b) validation by Western blot. Validation of selected interactions across all mutants of CDK4 by affinity purification coupled to Western blots.

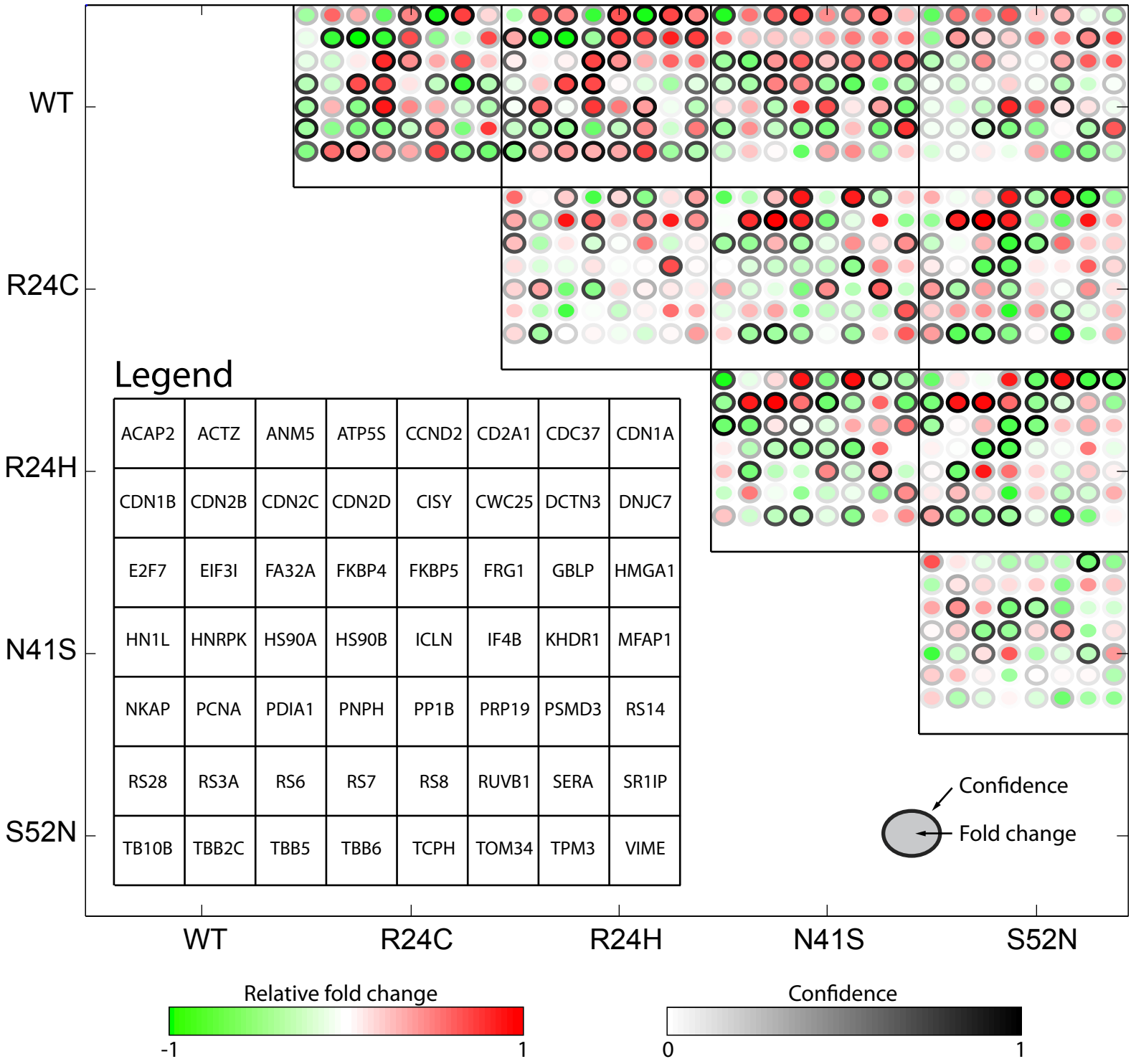

Supplementary Figure 20. Global view of the CDK4 dataset shown in Sup. Fig. 19 (group 2). Pairwise comparisons for the entire dataset. Only data for proteins with a Fold Change confidence ≥ 0.75 (and that have passed the other filters as described in Methods) in at least one pairwise comparison are displayed. The proteins are arranged in the matrix by decreasing confidence (across the entire dataset) in the same order for all comparisons (see legend). Relative Fold Change is displayed by the inside color of the circles (green to red scale). Confidence values are shown by the grey shading of the circle outline. Protein names are as per Uniprot; See Supplementary Table 1 for Official Gene Symbols and aliases.

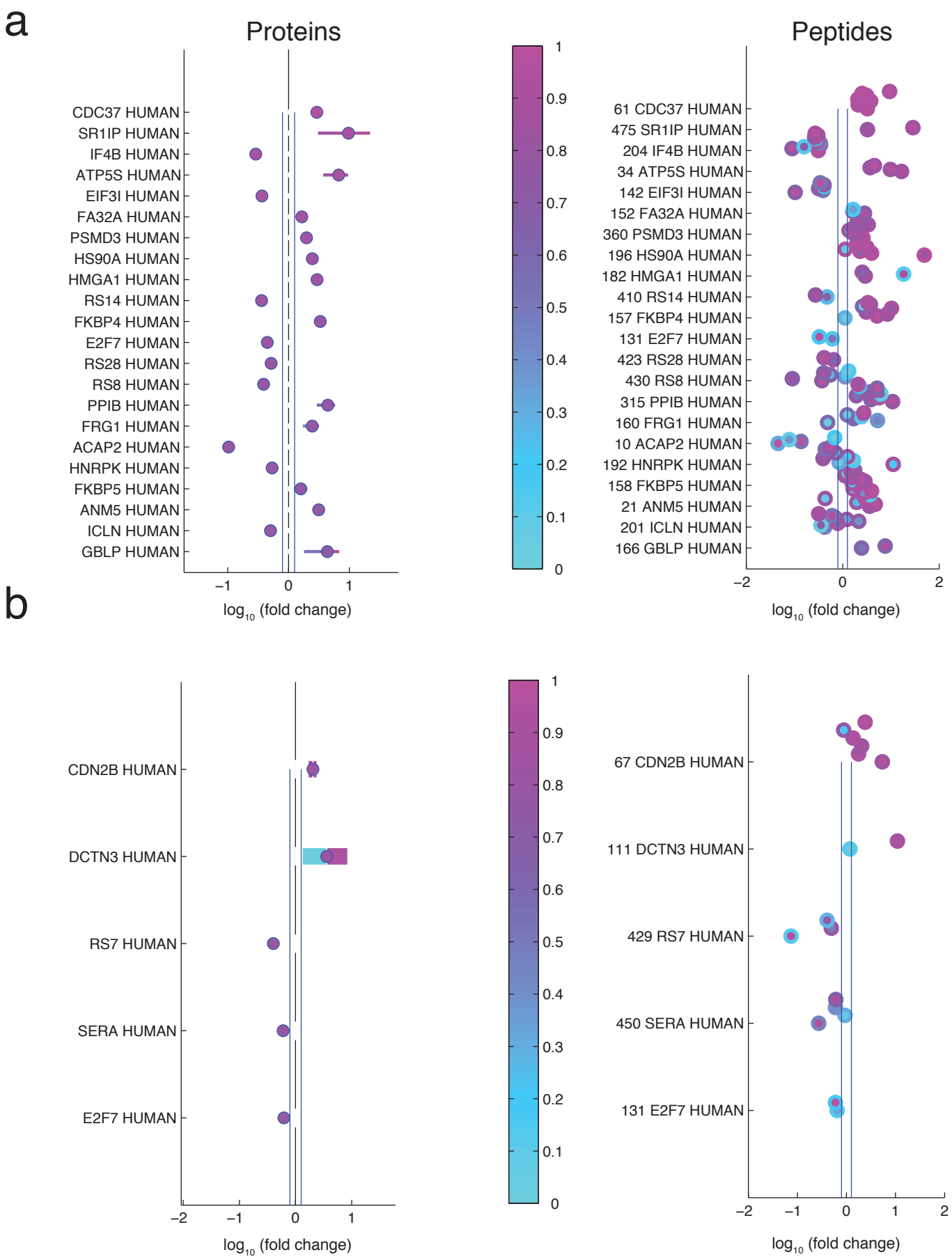

Supplementary Figure 21. Fold Change and confidence scores for the comparison of the CDK4 mutants N41S mutant (a) and the S52N mutant (b) to WT CDK4 (group 2). *Left panels*; protein Fold Change values where confidence is ≥ 0.75. *Right panels*; peptide level Fold Change with the confidence represented by the main colour and the signal-to-noise score by the outline colour. Labels are Uniprot protein names; see Supplementary Table 1 for Official Gene Symbols.

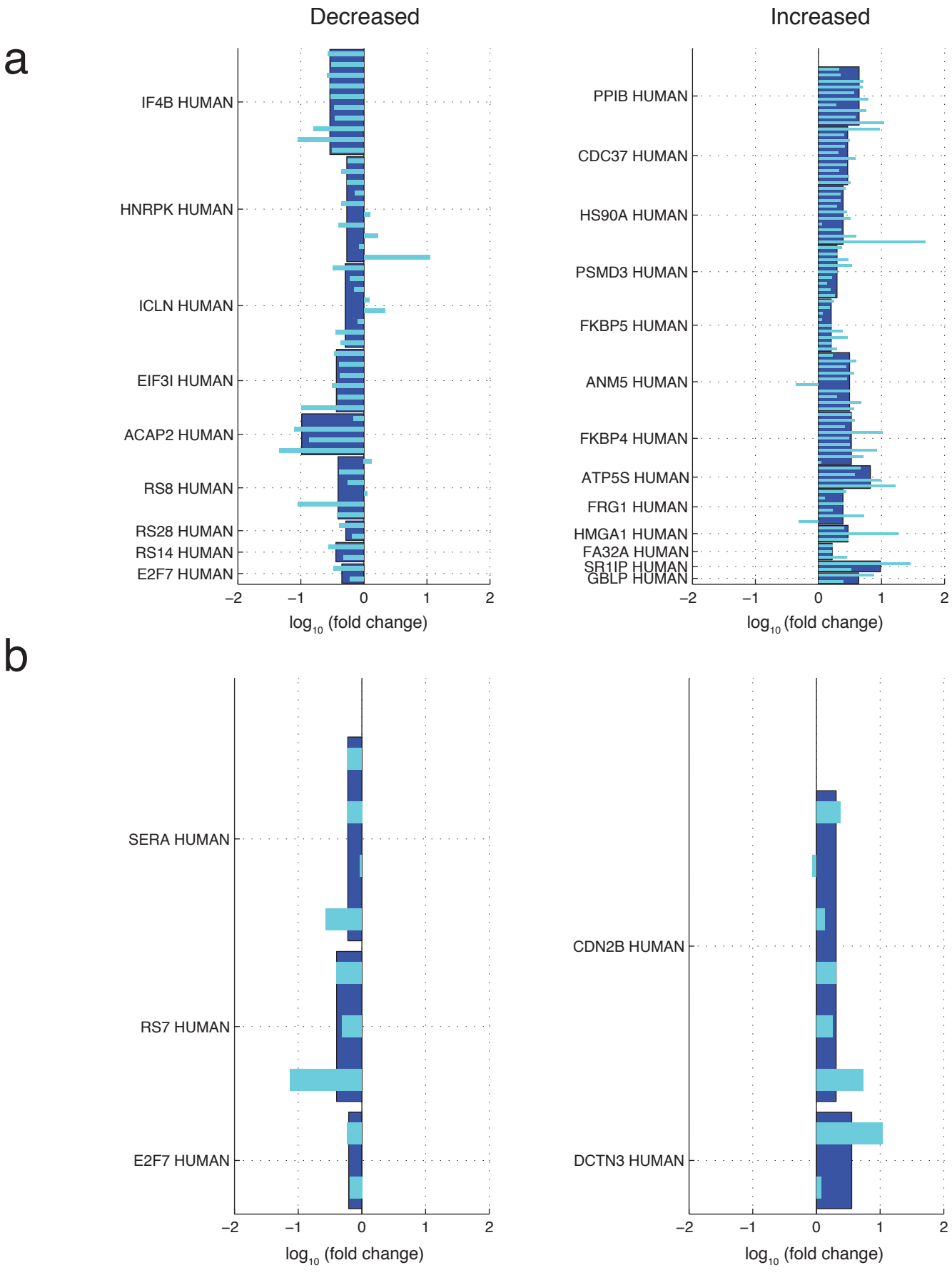

Supplementary Figure 22. Joint protein and peptide Fold Change for the comparison of the N41S (a) and S52N (b) mutants to WT CDK4 (group 2). *Left panel*; protein level and peptide level Fold Change for proteins identified with a confidence Fold Change ≥ 0.75 to be decreased in the mutants in comparison to the WT. *Right panel*; high confidence upregulated proteins. Labels are Uniprot protein names. The dark blue boxes are the protein Fold Changes, and the light blue are the peptides used for Fold Change calculation.

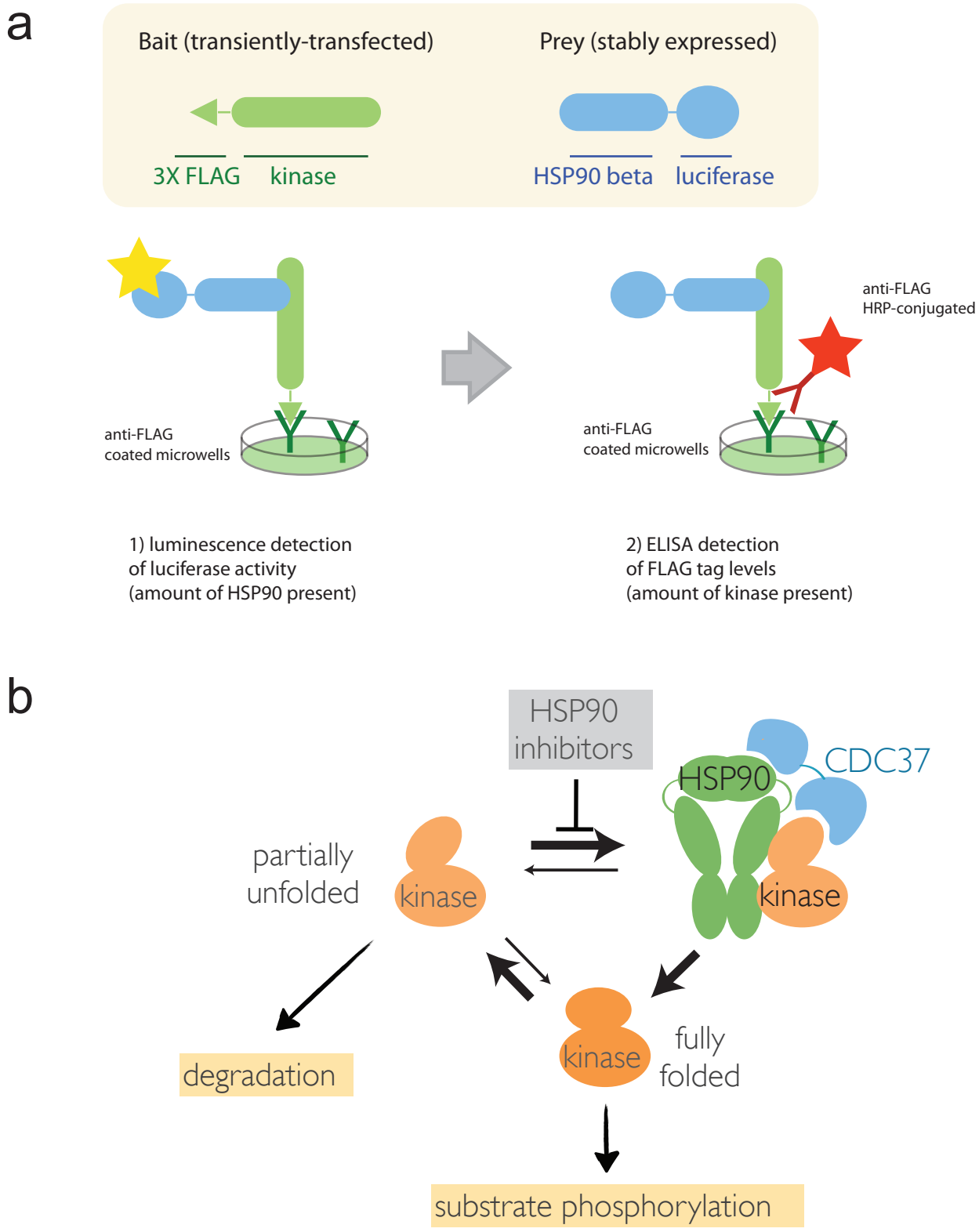

Supplementary Figure 23. LUMIER to detect HSP90 interactions and effects of HSP90 inhibitors on recruitment of kinases to HSP90-CDC37. a) Schematic of the LUMIER assay used here: a FLAG-tagged bait is transiently transfected in a stable cell line expressing HSP90 beta fused to luciferase. Cells are lysed, and the lysates are incubated on anti-FLAG coated well plates, rinsed, and subjected to luminescence detection of luciferase activity. Subsequently, the wells are washed, incubated with an anti-FLAG antibody conjugated to horseradish peroxidase and the levels of the kinases are detected by ELISA for normalization. b) Model depicting the known effect of HSP90 inhibitors, such as NVP-AUY922, on kinase recruitment to CDC37-HSP90 and on kinase stability.

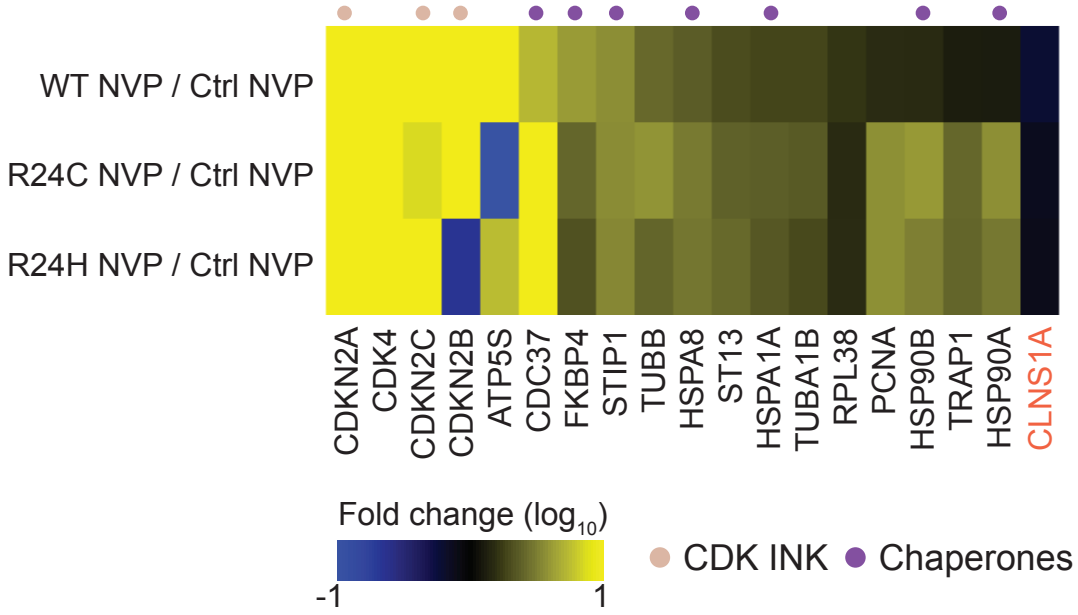

Supplementary Figure 24. Heatmap of the Fold Change for the CDK4 WT and mutants samples in comparison to a negative control following inhibition of HSP90 (group 3). Heatmap representation of the hits passing the confidence threshold for the CDK4 baits (WT, R24C and R24H) in comparison to the negative empty FLAG controls when treated with 500nM NVP-AUY922 for 1 hour.

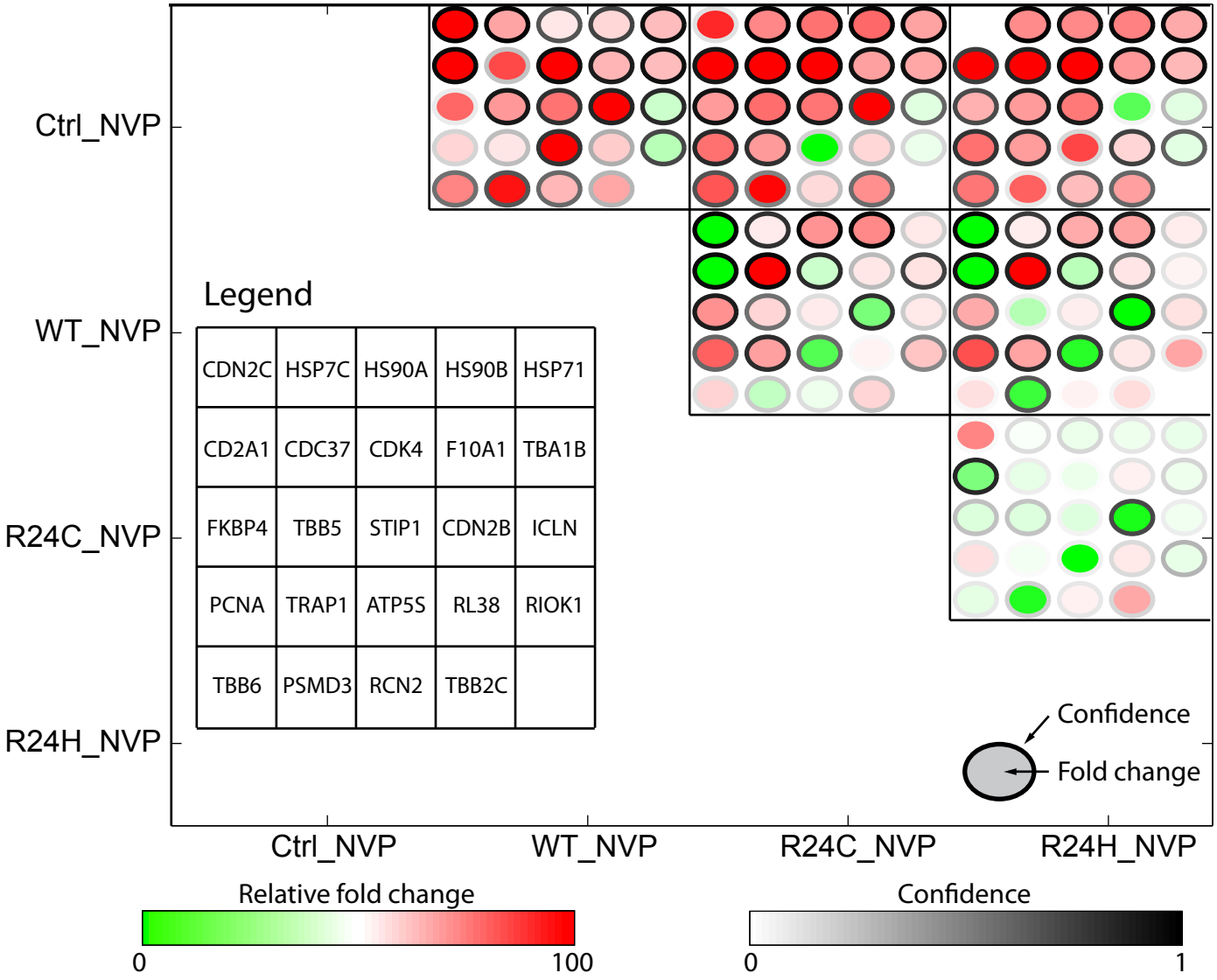

Supplementary Figure 25. Global view of the changes imparted by treatment with the HSP90 inhibitor NVP-AUY922 on protein-protein interactions shown in Fig. 5b (group 3). Pairwise comparisons for the entire dataset. Only data for proteins with a Fold Change confidence ≥ 0.75 (and that have passed the other filters as described in Methods) in at least one pairwise comparison are displayed. The proteins are arranged by decreasing confidence (across the entire dataset) in the same order for all comparisons (see legend). Relative Fold Change values are displayed by the inside color of the circles (green to red scale). Confidence values are shown by the grey shading of the circle outline. Protein names are as per Uniprot; See Supplementary Table 1 for Official Gene Symbols and aliases.

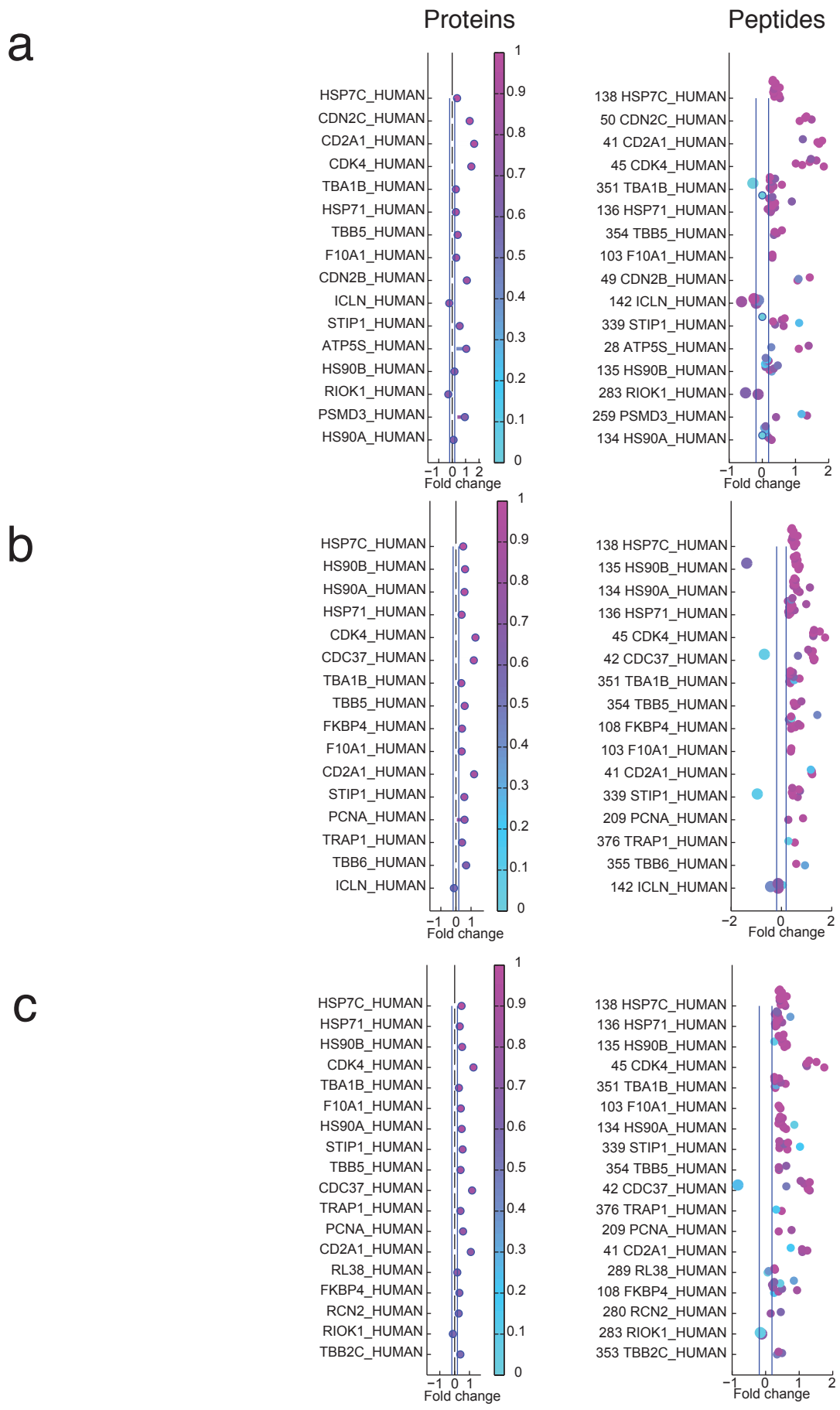

Supplementary Figure 26. Fold Changes and confidence scores for the comparison of the CDK4 (WT (a), R24C (b), R24C (c)) to a FLAG alone negative control upon HSP90 inhibition. *Left panels*; protein Fold Change values where confidence is ≥ 0.75. *Right panels*; peptide level Fold Change with the confidence represented by the main colour and the signal-to-noise score by the outline colour. Labels are Uniprot protein names; see Supplementary Table 1 for Official Gene Symbols.

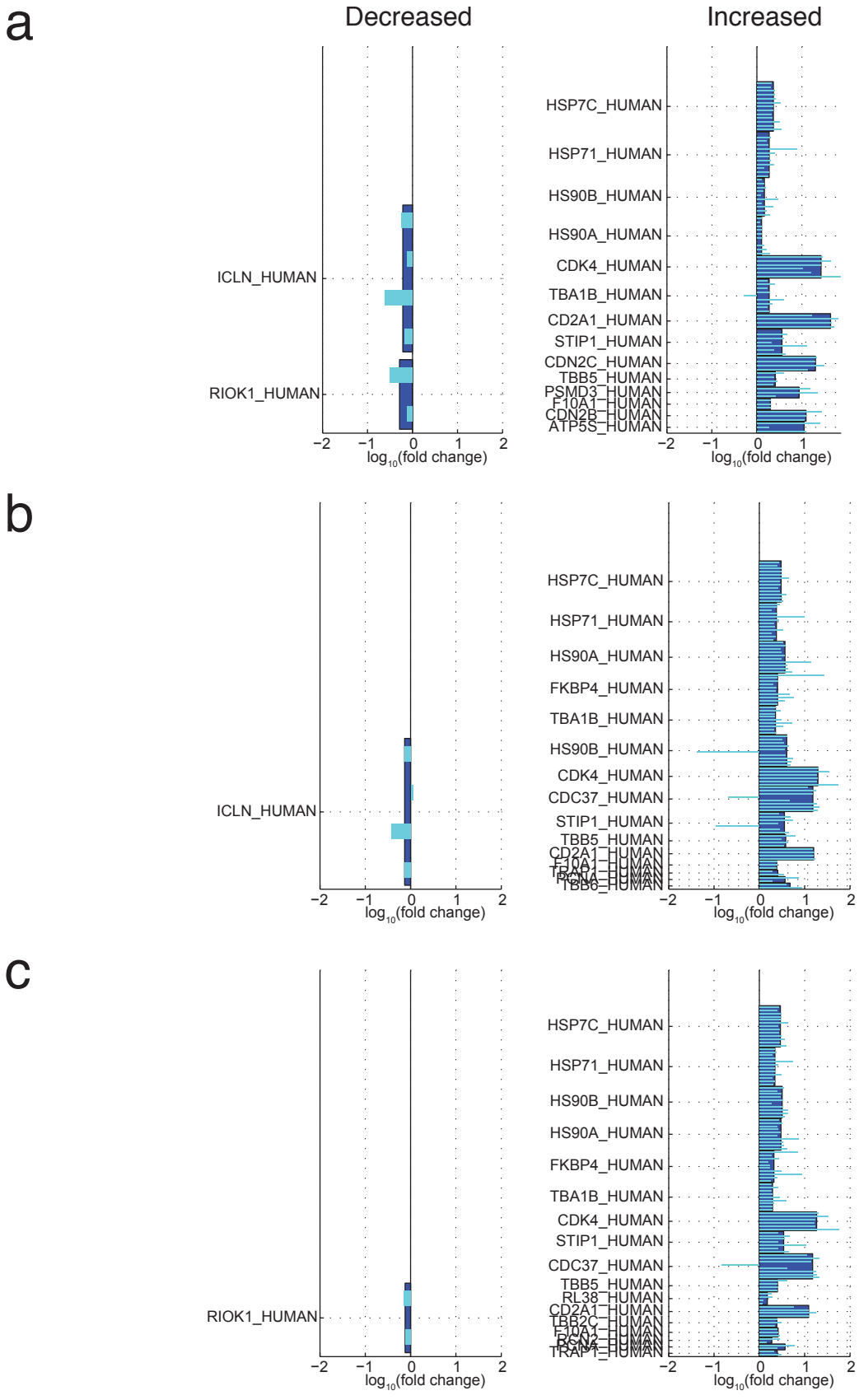

Supplementary Figure 27. Histogram representation of protein and peptide Fold Change induced by HSP90 inhibition for CDK4 WT (a), R24C (b) and R24H (c) (group 3). *Left panel*; protein level and peptide level Fold Change for proteins identified with a confidence Fold Change ≥ 0.75 to be decreased in the mutants in comparison to the B variant. *Right panel*; high confidence upregulated proteins. Labels are Uniprot protein names. The dark blue boxes are the protein Fold Changes, and the light blue are the peptides used for Fold Change calculation.

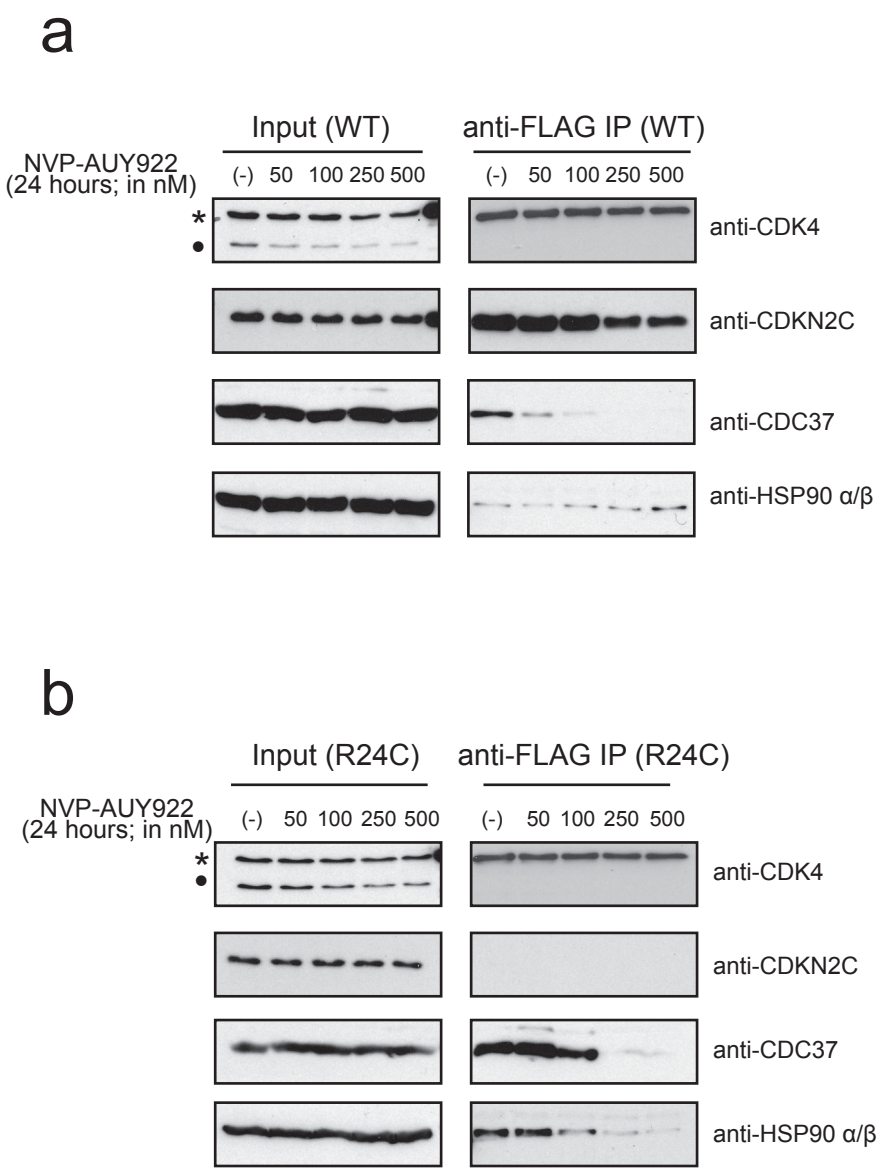

Supplementary Figure 28. AP-Western dose curve analysis of CDK4 WT (a) and R24C mutant (b) dissociation from CDC37-HSP90 in the presence of NVP-AUY922 for 24 hours. * indicates the position of the FLAG-tagged bait protein; • indicates endogenous CDK4.

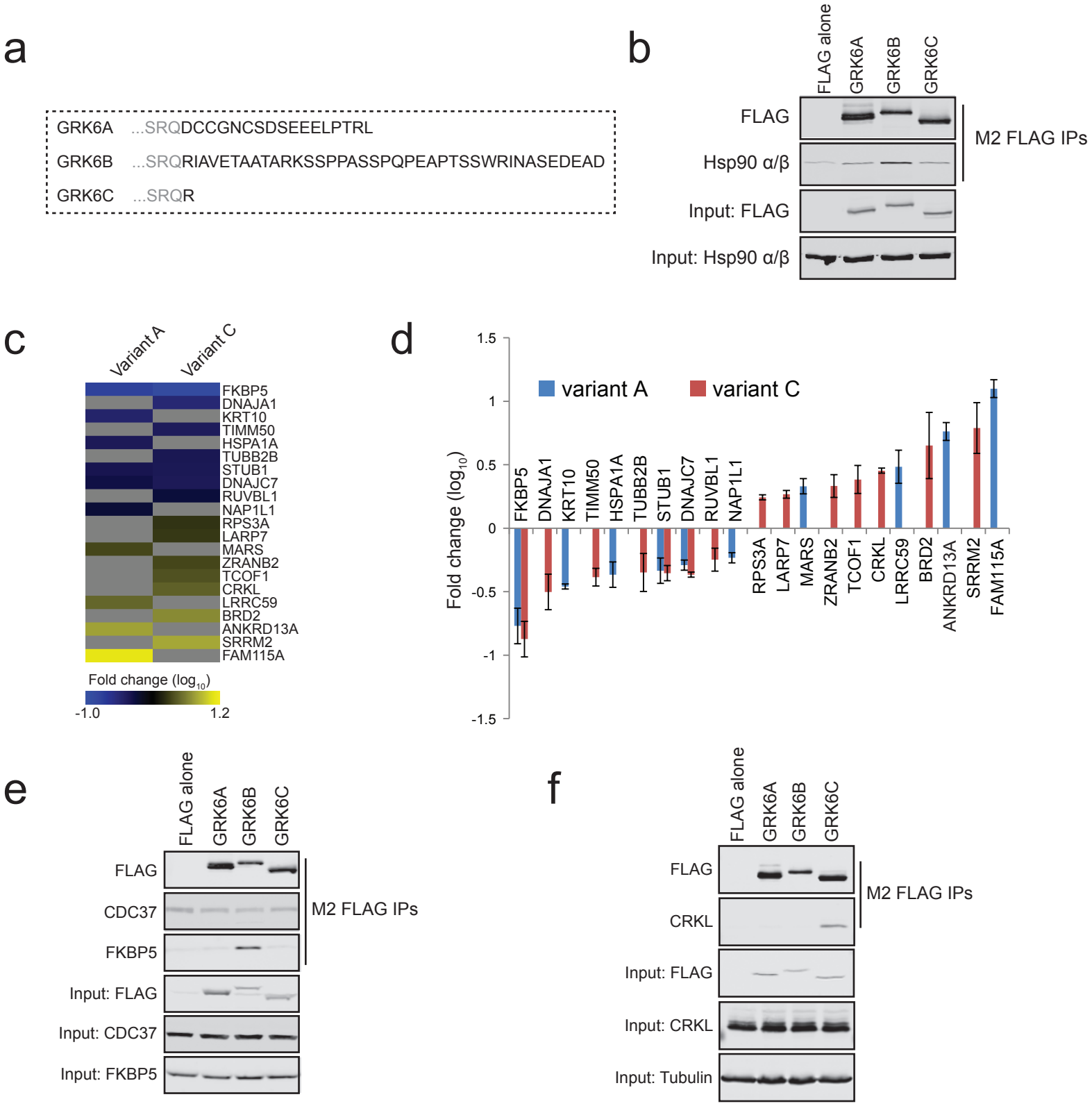

Supplementary Figure 29. Fold change analysis for the GRK6 dataset and validation by IP-western. a) Splice variants for the kinase GRK6 ony differ in their C-terminal tail. b) GRK6 splice variants differentially interact with HSP90, a protein also weakly interacting with the affinity resin. c) Identification of differential interactomes for GRK6 splice variants. High confidence (≥ 0.75) proteins displaying differential abundance in the A or C samples relative to the B sample; Supplementary Fig. 30 for all pairwise comparisons. d) Fold Change and Median Absolute Variance for selected proteins from panel c. See Supplementary Fig. 31-32 for an expanded view of protein and peptide level changes. e, f) Validation of interactions between FKBP52 (FKBP5) and GRK6 isoform B and between the GRK6 isoform C and the RTK scaffold CRKL.

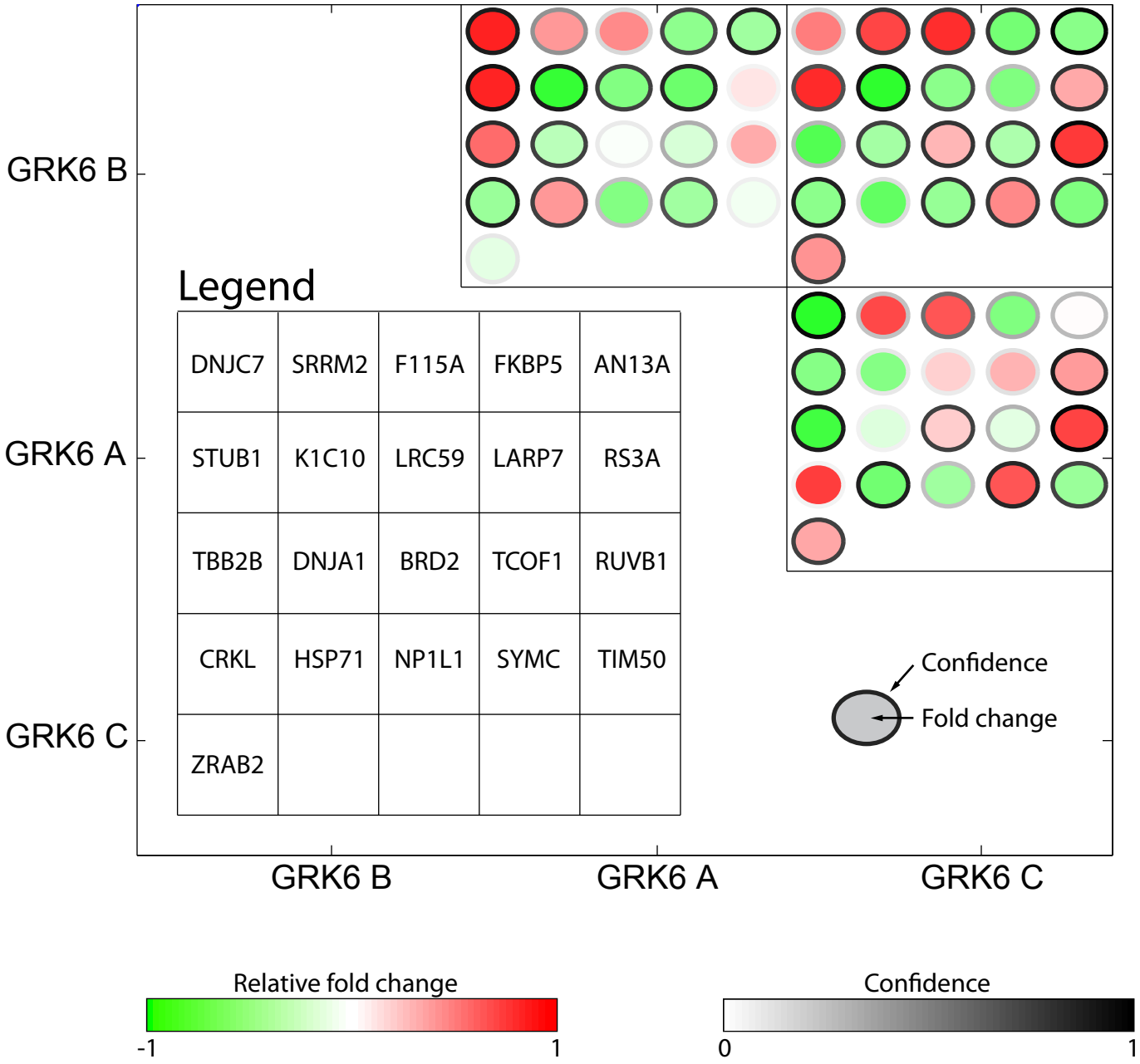

Supplementary Figure 30. Global view of the GRK6 splice variant dataset displayed in Sup. Fig. 29 (group 4). Pairwise comparisons for the entire dataset. Only data for proteins with a Fold Change confidence ≥ 0.75 (and that have passed the other filters as described in Methods) in at least one pairwise comparison are displayed. The proteins are arranged in the matrix by decreasing confidence (across the entire dataset) in the same order for all comparisons (see legend). Relative Fold Change is displayed by the inside color of the circles (green to red scale). Confidence values are shown by the grey shading of the circle outline. Protein names are as per Uniprot; See Supplementary Table 1 for Official Gene Symbols and aliases.

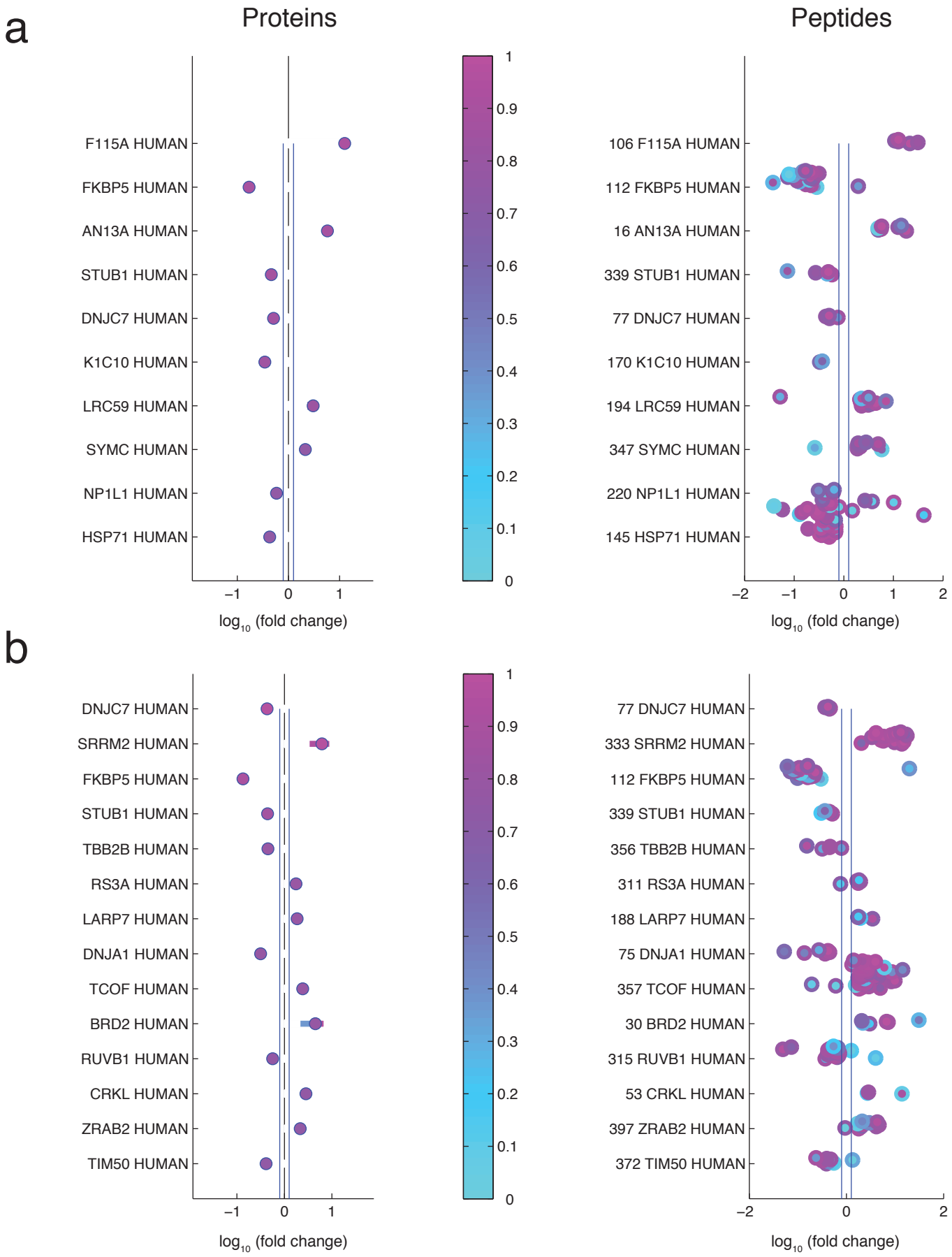

Supplementary Figure 31. Fold Changes and confidence scores for the comparison of the A variant (a) and the C variant (b) to the GRK6 splice variant B (group 4). *Left panels*; protein Fold Change values where confidence is ≥ 0.75. *Right panels*; peptide level Fold Change with the confidence represented by the main colour and the signal-to-noise score by the outline colour. Labels are Uniprot protein names; see Supplementary Table 1 for Official Gene Symbols.

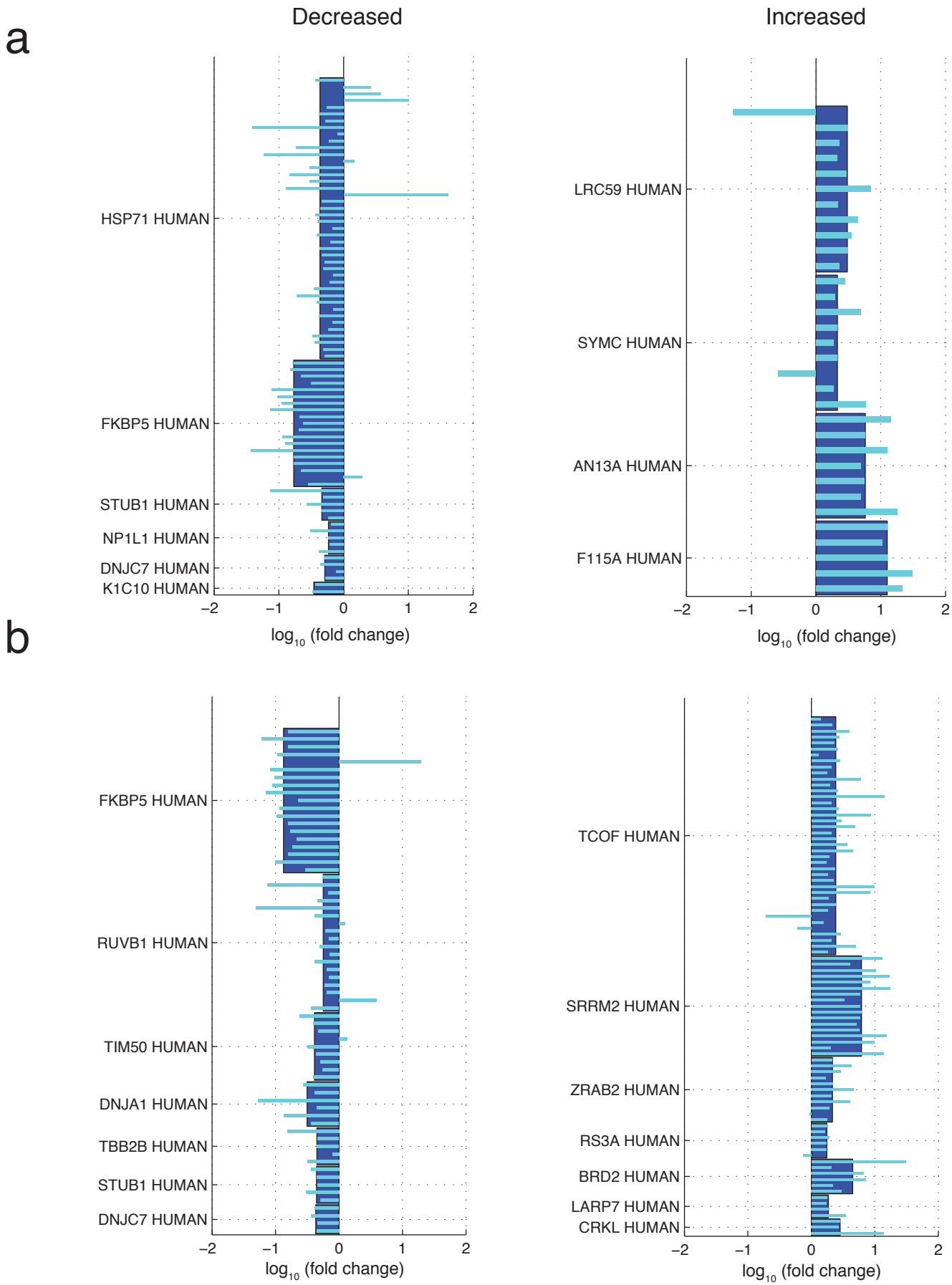

Supplementary Figure 32. Joint protein and peptide Fold Change for the comparison of the A (a) and C (b) variants to the B splice variant of GRK6 (group 4). *Left panel*; protein level and peptide level Fold Change for proteins identified with a confidence Fold Change ≥ 0.75 to be decreased in the mutants in comparison to the B variant. *Right panel*; high confidence upregulated proteins. Labels are Uniprot protein names. The dark blue boxes are the protein Fold Changes, and the light blue are the peptides used for Fold Change calculation.

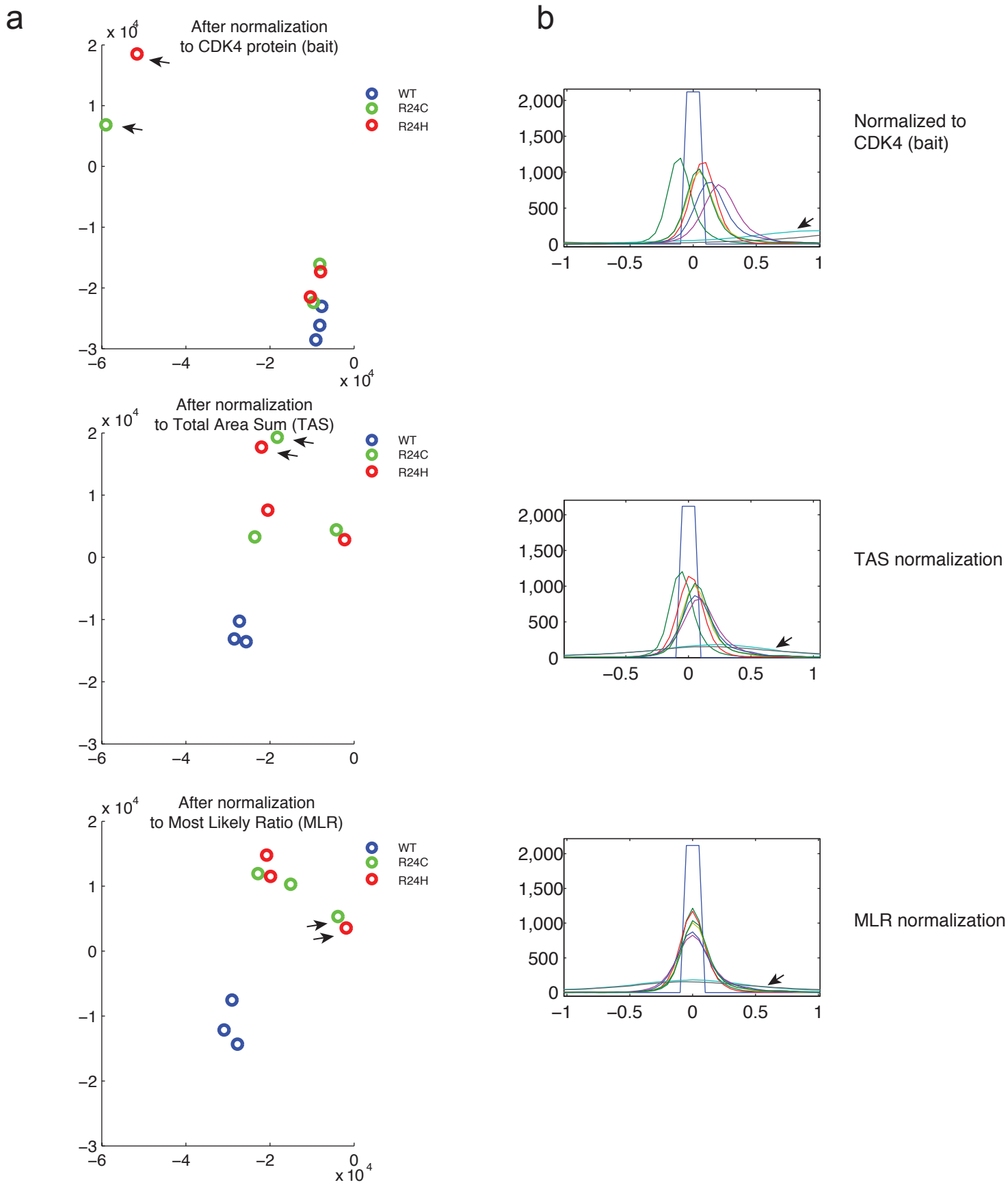

Supplementary Figure 33. Evaluation of the method of normalization using a CDK4 series (WT, R24C, R24H, all in triplicates) for which the intensities in one of each mutants were much lower than the other two. a) PCA analysis showing the sample groupings after different normalization methods; b) Area ratio histograms displaying the consequences of different methods of normalization on alignment improvement. For both panels: *top* displays the results of normalization based on the bait protein, *middle* shows the TAS normalization results, *bottom* shows the MLR results. The two samples which showed a reduced intensity in the dataset (samples 4 and 7 in Sup. Fig. 7) are marked with arrows.

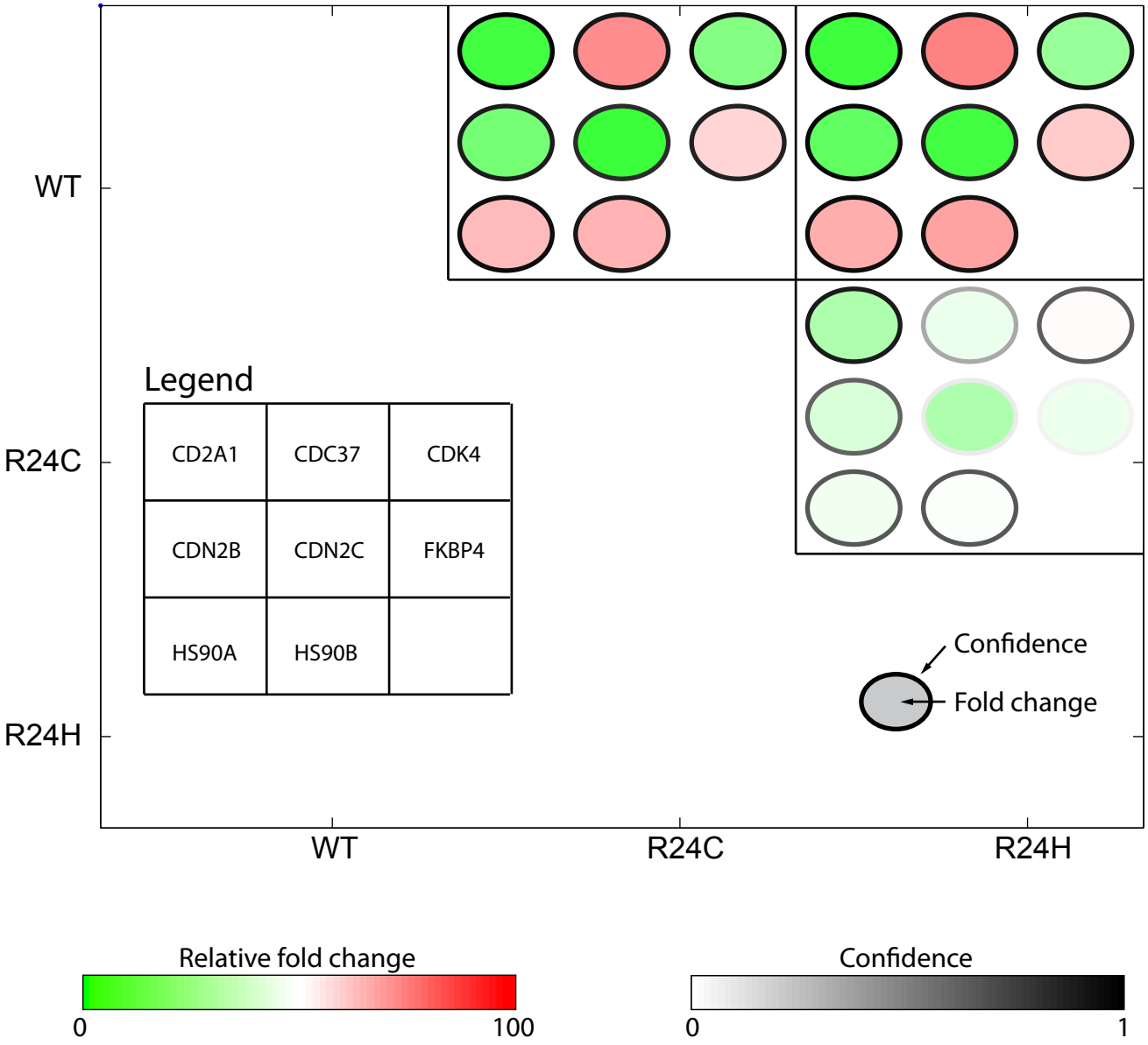

Supplementary Figure 34: Global view of CDK4 dataset containing 9 replicates for each bait (group 5). Pairwise comparisons for the entire dataset. Only data for proteins with a Fold Change confidence ≥ 0.75 (and that have passed the other filters as described in Methods) in at least one pairwise comparison are displayed. The proteins are arranged in the matrix by decreasing confidence (across the entire dataset) in the same order for all comparisons (see legend). Relative Fold Change values are displayed by the inside color of the circles (green to red scale). Confidence values are shown by the grey shading of the circle outline. Protein names are as per Uniprot; See Supplementary Table 1 for Official Gene Symbols and aliases.

a

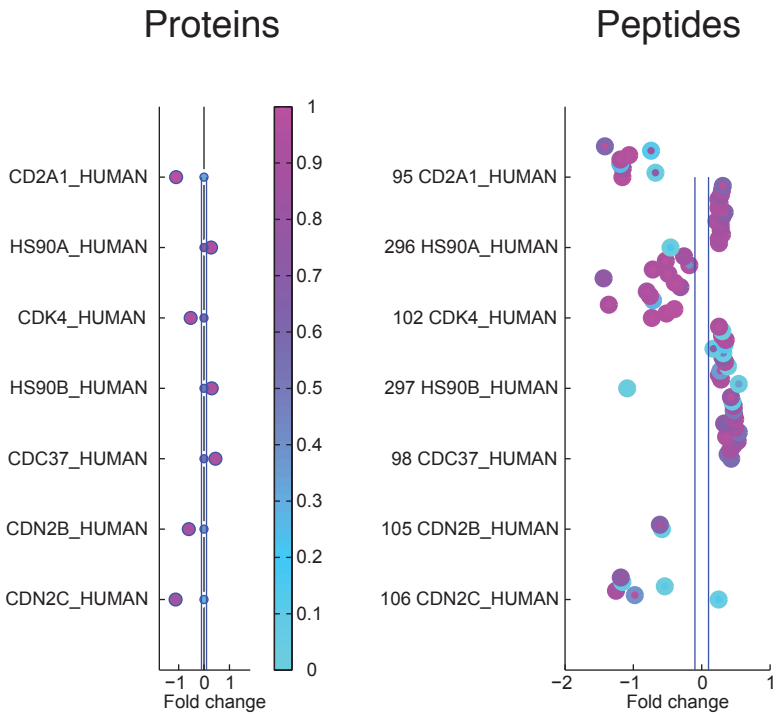

b

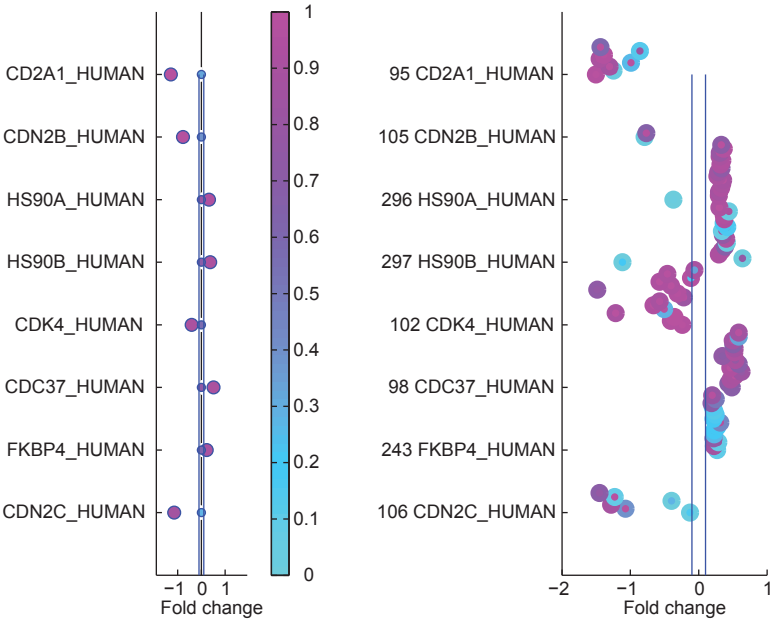

Supplementary Figure 35. Fold Changes and confidence scores for the comparison of CDK4 mutants (R24C (a), R24H mutant (b); 9 replicates each) to WT CDK4 (group 5). *Left panels*; protein Fold Change values where confidence is ≥ 0.75. *Right panels*; peptide level Fold Change with the confidence represented by the main colour and the signal-to-noise score by the outline colour. Labels are Uniprot protein names; see Supplementary Table 1 for Official Gene Symbols.

a

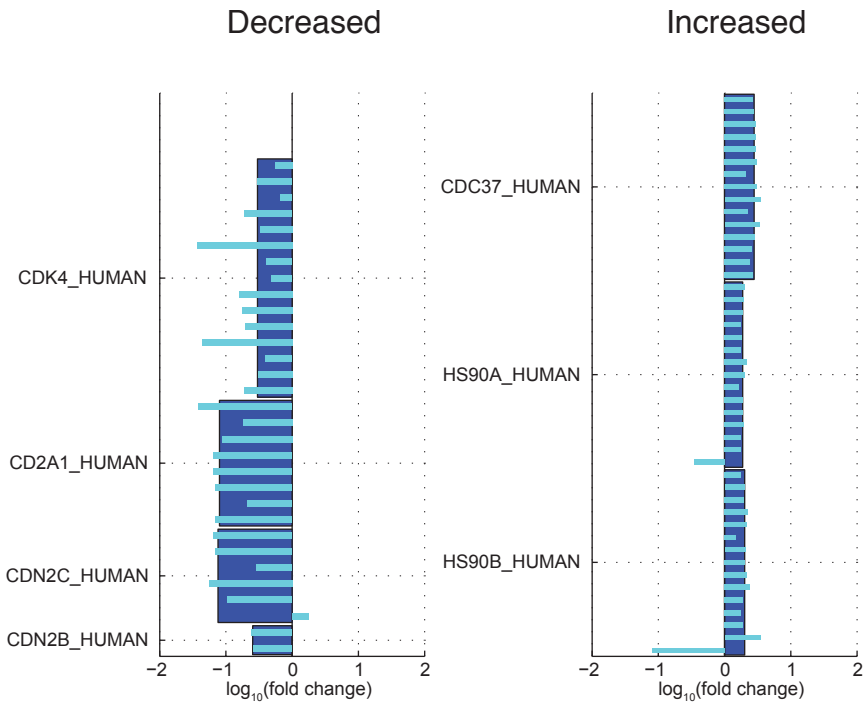

b

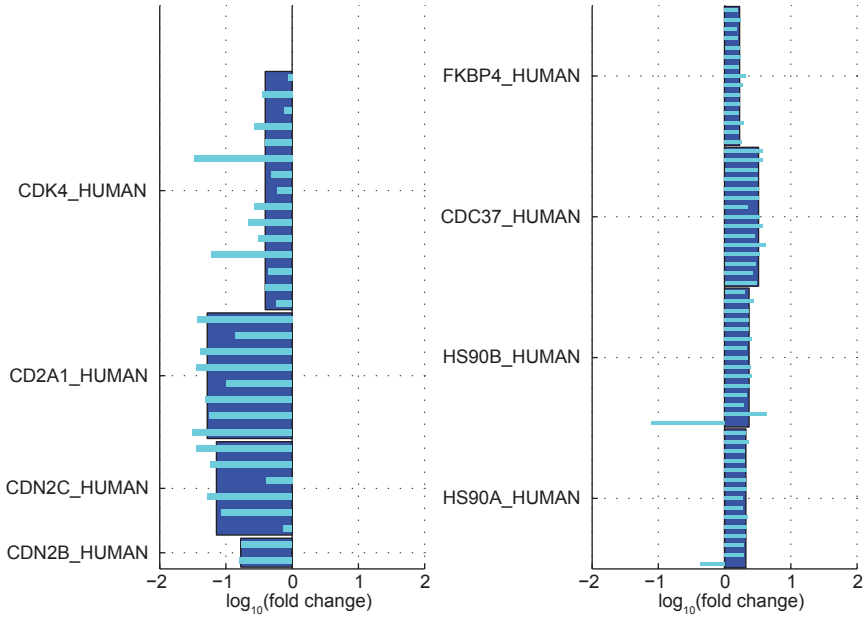

Supplementary Figure 36. Histogram representation of protein and peptide Fold Change of the R24 mutants (9 replicates; R24C (a), R24H (b)) to WT CDK4 (group 5). *Left panel*; protein level and peptide level Fold Change for proteins identified with a confidence Fold Change ≥ 0.75 to be decreased in the mutants in comparison to WT CDK4. *Right panel*; high confidence upregulated proteins. Labels are Uniprot protein names. The dark blue boxes are the protein Fold Changes, and the light blue are the peptides used for Fold Change calculation.

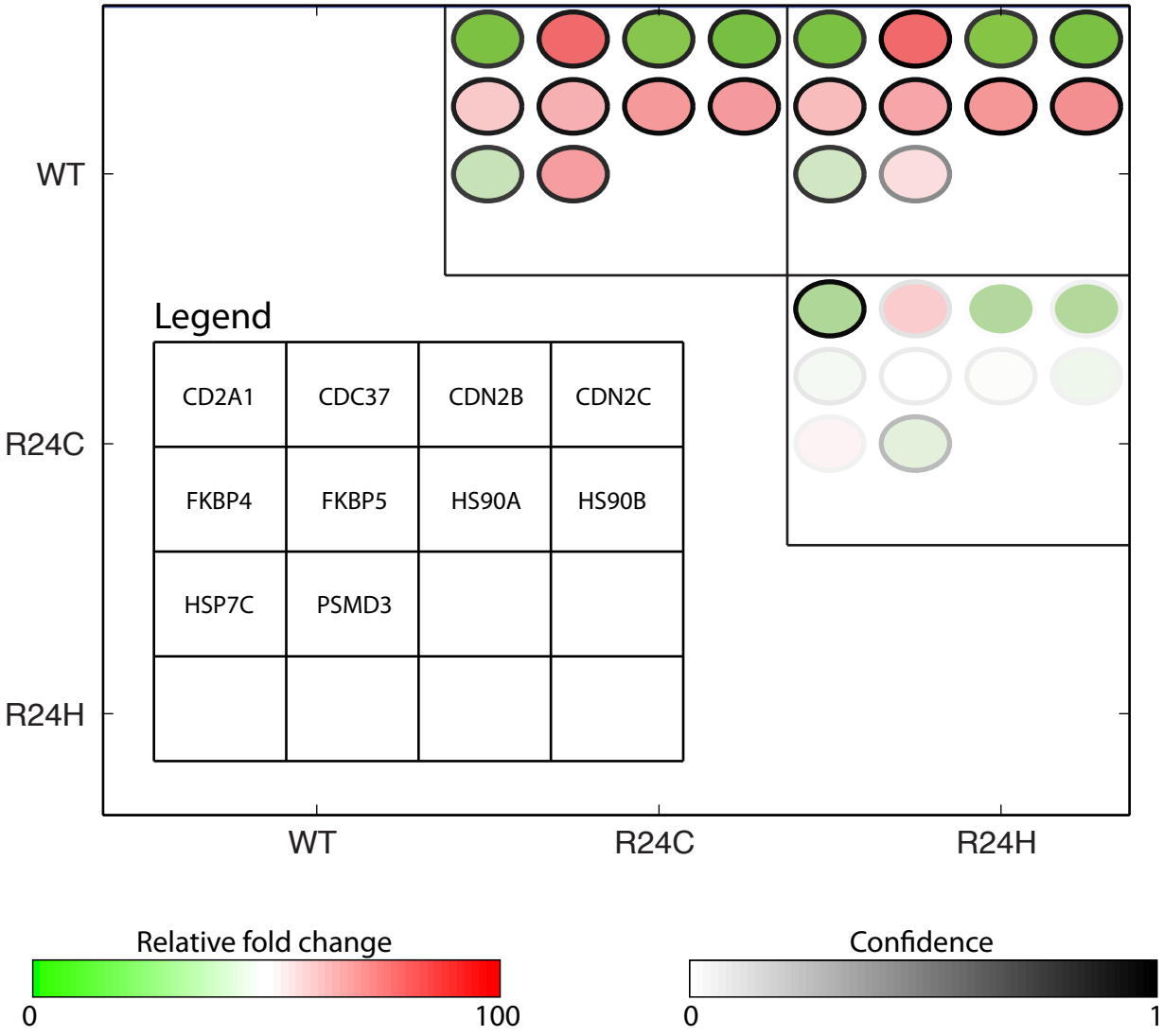

Supplementary Figure 37. Global view of CDK4 dataset containing 3 replicates for each bait (2011; group 1). Pairwise comparisons for the entire dataset. Only data for proteins with a Fold Change confidence ≥ 0.75 (and that have passed the other filters as described in Methods) in at least one pairwise comparison are displayed. The proteins are arranged in the matrix by decreasing confidence (across the entire dataset) in the same order for all comparisons (see legend). Relative Fold Change values are displayed by the inside color of the circles (green to red scale). Confidence values are shown by the grey shading of the circle outline. Protein names are as per Uniprot; See Supplementary Table 1 for Official Gene Symbols and aliases.

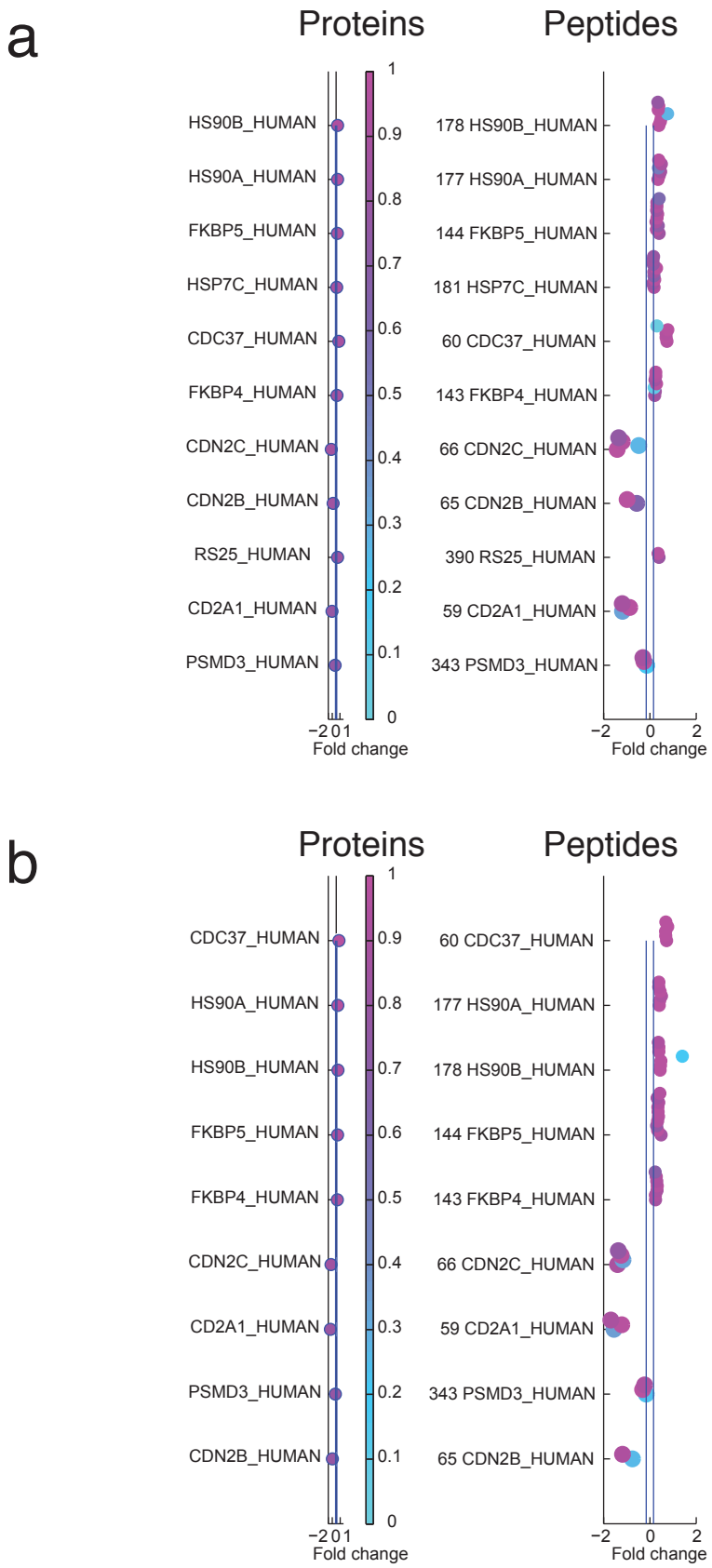

Supplementary Figure 38. Fold Changes and confidence scores for comparison of the R24 mutants (triplicates; R24C (a), R24H (b)) to WT CDK4 (group 1). *Left panels*; protein Fold Change values where confidence is ≥ 0.75. *Right panels*; peptide level Fold Change with the confidence represented by the main colour and the signal-to-noise score by the outline colour. Labels are Uniprot protein names; see Supplementary Table 1 for Official Gene Symbols.

a

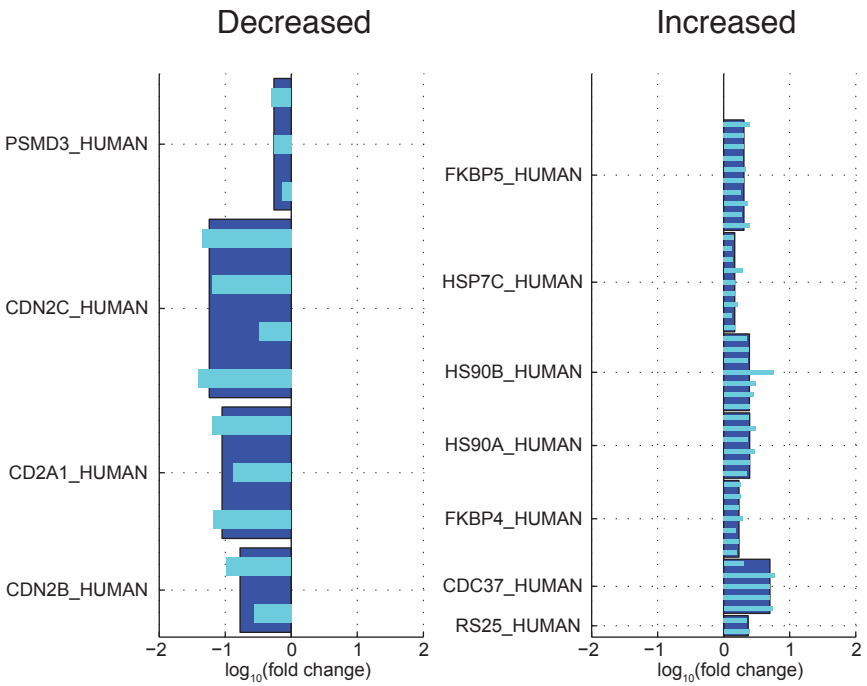

b

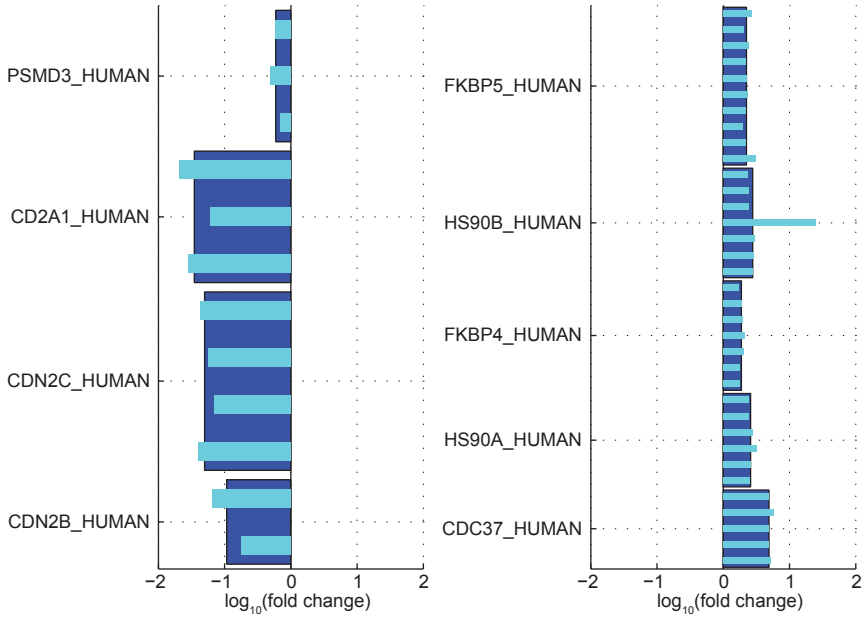

Supplementary Figure 39: Histogram representation of protein and peptide Fold Change of the R24 mutants (triplicates; R24C (a), R24H (b)) compared to the WT CDK4 (group 1). *Left panel*; protein level and peptide level Fold Change for proteins identified with a confidence Fold Change ≥ 0.75 to be decreased in the mutants in comparison to CDK4 WT. *Right panel*; high confidence upregulated proteins. Labels are Uniprot protein names. The dark blue boxes are the protein Fold Changes, and the light blue are the peptides used for Fold Change calculation.

Supplementary Table 1. List of Official Gene Symbols, Uniprot Names, and common aliases used in this study for key proteins in the network.

Gene Symbol	Uniprot Accession	Alias used	Recommended name (Uniprot)
ACAP2	ACAP2_HUMAN		Arf-GAP with coiled-coil, ANK repeat and PH domain-containing protein 2
ACTR1A	ACTZ_HUMAN		Alpha-centractin
ANKRD13A	AN13A_HUMAN		Ankyrin repeat domain-containing protein 13A
PRMT5	ANM5_HUMAN		Protein arginine N-methyltransferase 5
ATP5S	ATP5S_HUMAN		ATP synthase subunit s, mitochondrial
BRD2	BRD2_HUMAN		Bromodomain-containing protein 2
C1QBP	C1QBP_HUMAN		Complement component 1 Q subcomponent-binding protein
CCND2	CCND2_HUMAN		G1/S-specific cyclin-D2
CDKN2A	CD2A1_HUMAN	p16INK	Cyclin-dependent kinase inhibitor 2A, isoforms 1/2/3
CDC37	CDC37_HUMAN		Hsp90 co-chaperone Cdc37
CDK4	CDK4_HUMAN		Cyclin-dependent kinase 4
CDK9	CDK9_HUMAN		Cyclin-dependent kinase 9
CDKN1A	CDN1A_HUMAN		Cyclin-dependent kinase inhibitor 1
CDKN1B	CDN1B_HUMAN	p27KIP1	Cyclin-dependent kinase inhibitor 1B
CDKN2B	CDN2B_HUMAN	p15INK	Cyclin-dependent kinase 4 inhibitor B
CDKN2C	CDN2C_HUMAN	p18INK	Cyclin-dependent kinase 4 inhibitor C
CDKN2D	CDN2D_HUMAN	p19INK	Cyclin-dependent kinase 4 inhibitor D (p19-INK4d)
CIRBP	CIRBP_HUMAN		Cold-inducible RNA-binding protein
CS	CISY_HUMAN		Citrate synthase, mitochondrial
CRKL	CRKL_HUMAN		Crk-like protein
CWC25	CWC25_HUMAN		Pre-mRNA-splicing factor CWC25 homolog
DCTN3	DCTN3_HUMAN		Dynactin subunit 3
DDX3X	DDX3X_HUMAN		ATP-dependent RNA helicase DDX3X
DNAJB6	DNJA1_HUMAN		DnaJ homolog subfamily A member 1
DNAJC7	DNJC7_HUMAN		DnaJ homolog subfamily C member 7
E2F7	E2F7_HUMAN		Transcription factor E2F7
EIF3A	EIF3A_HUMAN		Eukaryotic translation initiation factor 3 subunit A
EIF3B	EIF3B_HUMAN		Eukaryotic translation initiation factor 3 subunit B
EIF3C	EIF3C_HUMAN		Eukaryotic translation initiation factor 3 subunit C
EIF3E	EIF3E_HUMAN		Eukaryotic translation initiation factor 3 subunit E
EIF3F	EIF3F_HUMAN		Eukaryotic translation initiation factor 3 subunit F
EIF3H	EIF3H_HUMAN		Eukaryotic translation initiation factor 3 subunit H
EIF3I	EIF3I_HUMAN		Eukaryotic translation initiation factor 3 subunit I
EIF3M	EIF3M_HUMAN		Eukaryotic translation initiation factor 3 subunit M
ST13	F10A1_HUMAN	HIP	Hsc70-interacting protein
FAM115A	F115A_HUMAN		Protein FAM115A
FAM32A	FA32A_HUMAN		Protein FAM32A
FKBP4	FKBP4_HUMAN	FKBP51	Peptidyl-prolyl cis-trans isomerase FKBP4
FKBP5	FKBP5_HUMAN	FKBP52	Peptidyl-prolyl cis-trans isomerase FKBP5
FRG1	FRG1_HUMAN		Protein FRG1
GNB2L1	GBLP_HUMAN		Guanine nucleotide-binding protein subunit beta-2-like 1
HIST1H1C	H12_HUMAN		Histone H1.2
HMGA1	HMGA1_HUMAN		High mobility group protein HMG-I/HMG-Y
HN1L	HN1L_HUMAN		Hematological and neurological expressed 1-like protein
HNRNPK	HNRPK_HUMAN		Heterogeneous nuclear ribonucleoprotein K
HSP90AA1	HS90A_HUMAN	HSP90 alpha	Heat shock protein HSP 90-alpha
HSP90AB1	HS90B_HUMAN	HSP90 beta	Heat shock protein HSP 90-beta
HSPA1A	HSP71_HUMAN	HSP70 1/2	Heat shock 70 kDa protein 1A/1B
HSPA8	HSP7C_HUMAN		Heat shock cognate 71 kDa protein
CLNS1A	ICLN_HUMAN		Methylosome subunit pICln
EIF1AX	IF1AX_HUMAN		Eukaryotic translation initiation factor 1A, X-chromosomal

EIF3L	IF3EI_HUMAN	Eukaryotic translation initiation factor 3 subunit L
EIF4A2	IF4A2_HUMAN	Eukaryotic initiation factor 4A-II
EIF4B	IF4B_HUMAN	Eukaryotic translation initiation factor 4B
EIF4G1	IF4G1_HUMAN	Eukaryotic translation initiation factor 4 gamma 1
EIF4G2	IF4G2_HUMAN	Eukaryotic translation initiation factor 4 gamma 2
EIF4G3	IF4G3_HUMAN	Eukaryotic translation initiation factor 4 gamma 3
KPNA3	IMA3_HUMAN	Importin subunit alpha-3
KPNB1	IMB1_HUMAN	Importin subunit beta-1
IRS4	IRS4_HUMAN	Insulin receptor substrate 4
KRT5	K1C10_HUMAN	Keratin, type I cytoskeletal 10
KHDRBS1	KHDR1_HUMAN	KH domain-containing, RNA-binding, signal transduction-associated protein 1
SSB	LA_HUMAN	Lupus La protein
LARP7	LARP7_HUMAN	La-related protein 7
LRRC59	LRC59_HUMAN	Leucine-rich repeat-containing protein 59
MEPCE	MEPCE_HUMAN	7SK snRNA methylphosphate capping enzyme
MFAP1	MFAP1_HUMAN	Microfibrillar-associated protein 1
NKAP	NKAP_HUMAN	NF-kappa-B-activating protein
NAP1L1	NP1L1_HUMAN	Nucleosome assembly protein 1-like 1
NPM1	NPM_HUMAN	Nucleophosmin
ENDOG	NUCG_HUMAN	Endonuclease G, mitochondrial
PABPC1	PABP1_HUMAN	Polyadenylate-binding protein 1
PCNA	PCNA_HUMAN	Proliferating cell nuclear antigen
PDCD4	PDCD4_HUMAN	Programmed cell death protein 4
P4HB	PDIA1_HUMAN	Protein disulfide-isomerase
PNP	PNPH_HUMAN	Purine nucleoside phosphorylase
PPIB	PPIB_HUMAN	Peptidyl-prolyl cis-trans isomerase B
PRDX2	PRDX2_HUMAN	Peroxiredoxin-2
PRDX6	PRDX6_HUMAN	Peroxiredoxin-6
PRPF19	PRP19_HUMAN	Pre-mRNA-processing factor 19
PRPF4	PRP4_HUMAN	U4/U6 small nuclear ribonucleoprotein Prp4
PRPF3	PRPF3_HUMAN	U4/U6 small nuclear ribonucleoprotein Prp3
PSMC1	PRS4_HUMAN	26S protease regulatory subunit 4
PSMB3	PSB3_HUMAN	Proteasome subunit beta type-3
PSMB6	PSB6_HUMAN	Proteasome subunit beta type-6
PSMD11	PSD11_HUMAN	26S proteasome non-ATPase regulatory subunit 11
PSMD12	PSD12_HUMAN	26S proteasome non-ATPase regulatory subunit 12
PSMD13	PSD13_HUMAN	26S proteasome non-ATPase regulatory subunit 13
PSMD7	PSD7_HUMAN	26S proteasome non-ATPase regulatory subunit 7
PSMD14	PSDE_HUMAN	26S proteasome non-ATPase regulatory subunit 14
PSMD3	PSMD3_HUMAN	26S proteasome non-ATPase regulatory subunit 3
PSMD6	PSMD6_HUMAN	26S proteasome non-ATPase regulatory subunit 6
RAB11B	RB11B_HUMAN	Ras-related protein Rab-11B
RCN2	RCN2_HUMAN	Reticulocalbin-2
RIOK1	RIOK1_HUMAN	Serine/threonine-protein kinase RIO1
RPL11	RL11_HUMAN	60S ribosomal protein L11
RPL12	RL12_HUMAN	60S ribosomal protein L12
RPL13	RL13_HUMAN	60S ribosomal protein L13
RPL17	RL17_HUMAN	60S ribosomal protein L17
RPL18	RL18_HUMAN	60S ribosomal protein L18
RPL19	RL19_HUMAN	60S ribosomal protein L19
RPL26	RL26_HUMAN	60S ribosomal protein L26
RPL31	RL31_HUMAN	60S ribosomal protein L31
RPL35	RL35_HUMAN	60S ribosomal protein L35
RPL38	RL38_HUMAN	60S ribosomal protein L38
RPL4	RL4_HUMAN	60S ribosomal protein L4
RPLP0	RLA0_HUMAN	60S acidic ribosomal protein P0

HNRNPA1	ROA1_HUMAN		Heterogeneous nuclear ribonucleoprotein A1
RPS13	RS13_HUMAN		40S ribosomal protein S13
RPS14	RS14_HUMAN		40S ribosomal protein S14
RPS15A	RS15A_HUMAN		40S ribosomal protein S15a
RPS16	RS16_HUMAN		40S ribosomal protein S16
RPS19	RS19_HUMAN		40S ribosomal protein S19
RPS2	RS2_HUMAN		40S ribosomal protein S2
RPS20	RS20_HUMAN		40S ribosomal protein S20
RPS23	RS23_HUMAN		40S ribosomal protein S23
RPS24	RS24_HUMAN		40S ribosomal protein S24
RPS25	RS25_HUMAN		40S ribosomal protein S25
RPS28	RS28_HUMAN		40S ribosomal protein S28
RPS3	RS3_HUMAN		40S ribosomal protein S3
RPS3A	RS3A_HUMAN		40S ribosomal protein S3a
RPS4X	RS4X_HUMAN		40S ribosomal protein S4, X isoform
RPS6	RS6_HUMAN		40S ribosomal protein S6
RPS7	RS7_HUMAN		40S ribosomal protein S7
RPS8	RS8_HUMAN		40S ribosomal protein S8
RPS9	RS9_HUMAN		40S ribosomal protein S9
SNRPB	RSMB_HUMAN		Small nuclear ribonucleoprotein-associated proteins B and B'
RPSA	RSSA_HUMAN		40S ribosomal protein SA
RUVBL1	RUVB1_HUMAN		RuvB-like 1
SART3	SART3_HUMAN		Squamous cell carcinoma antigen recognized by T-cells 3
PHGDH	SERA_HUMAN		D-3-phosphoglycerate dehydrogenase
SET	SET_HUMAN		Protein SET
SNRPD1	SMD1_HUMAN		Small nuclear ribonucleoprotein Sm D1
SNRPD2	SMD2_HUMAN		Small nuclear ribonucleoprotein Sm D2
SREK1IP1	SR1IP_HUMAN		Protein SREK1IP1
SRRM2	SRRM2_HUMAN		SRRM2 protein
STIP1	STIP1_HUMAN	HOP	Stress-induced-phosphoprotein 1
STK38	STK38_HUMAN		Serine/threonine-protein kinase 38
STUB1	STUB1_HUMAN		E3 ubiquitin-protein ligase CHIP
MARS	SYMC_HUMAN		Methionine--tRNA ligase, cytoplasmic
TBC1D10B	TB10B_HUMAN		TBC1 domain family member 10B
TUBA1B	TBA1B_HUMAN		Tubulin alpha-1B chain
TUBB2B	TBB2B_HUMAN		Tubulin beta-2B chain
TUBB4B	TBB2C_HUMAN		Tubulin beta-4B chain
TUBB	TBB5_HUMAN		Tubulin beta chain
TUBB6	TBB6_HUMAN		Tubulin beta-6 chain
TCOF1	TCOF_HUMAN		Treacle protein
CCT7	TCPH_HUMAN		T-complex protein 1 subunit eta
CCT8	TCPQ_HUMAN		T-complex protein 1 subunit theta
TIMM13	TIM13_HUMAN		Mitochondrial import inner membrane translocase subunit Tim13
TIMM50	TIM50_HUMAN		Mitochondrial import inner membrane translocase subunit TIM50
TOMM34	TOM34_HUMAN		Mitochondrial import receptor subunit TOM34
TPM3	TPM3_HUMAN		Tropomyosin alpha-3 chain
TRAP1	TRAP1_HUMAN		Heat shock protein 75 kDa, mitochondrial
VIM	VIME_HUMAN		Vimentin
ZRANB2	ZRAB2_HUMAN		Zinc finger Ran-binding domain-containing protein 2 (Zinc finger protein 265)

Supplementary Table 2. Composition of the dataset and naming convention. Columns are as follows: "ProHits ID", unique identified from our LIMS; "Raw file name" refers to the name of the raw file as provided on the website; see Methods for the description of the "Chromatography system"; "Group file" indicates that a specific IDA file was used to create a given group file for peak extraction, and to indicate which group file was used for targeted extraction from the SWATH file. Group files are associated with separate "export" groups in the Lunenfeld-Tanenbaum instance of ProHits; these are the subject of different submissions to MassIVE. See Supplementary Table 4 for details and MassIVE IDs; also see prohits-web.lunenfeld.ca for additional details and access to Supplementary information.

ProHits ID	Acquisition	Set	Bait gene	Sequence variant	Treatment	Replicate	Short_label	Raw file name	Chromatography system	Group file
13988	IDA	CDK4_first_mutants	CDK4	R24C	none	2	R24C	13988_Cdk47ct_SLRIACG02_IDA.wiff	TrapElute-nanoflexTop50	1
14002	IDA	CDK4_first_mutants	CDK4	R24H	none	2	R24H	14002_Cdk467a_SLRIACG02_IDA.wiff	TrapElute-nanoflexTop50	1
13974	IDA	CDK4_first_mutants	CDK4	WT	none	2	WT	13974_Cdk4wt_SLRIACG02_IDA.wiff	TrapElute-nanoflexTop50	1
13987	SWATH	CDK4_first_mutants	CDK4	R24C	none	1	R24C	13987_Cdk47ct_SLRIACG01_Swath.wiff	TrapElute-nanoflexSwath	1
13989	SWATH	CDK4_first_mutants	CDK4	R24C	none	2	R24C	13989_Cdk47ct_SLRIACG02_Swath.wiff	TrapElute-nanoflexSwath	1
13991	SWATH	CDK4_first_mutants	CDK4	R24C	none	3	R24C	13991_Cdk47ct_SLRIACG03_Swath.wiff	TrapElute-nanoflexSwath	1
14001	SWATH	CDK4_first_mutants	CDK4	R24H	none	1	R24H	14001_Cdk467a_SLRIACG01_Swath.wiff	TrapElute-nanoflexSwath	1
14003	SWATH	CDK4_first_mutants	CDK4	R24H	none	2	R24H	14003_Cdk467a_SLRIACG02_Swath.wiff	TrapElute-nanoflexSwath	1
14005	SWATH	CDK4_first_mutants	CDK4	R24H	none	3	R24H	14005_Cdk467a_SLRIACG03_Swath.wiff	TrapElute-nanoflexSwath	1
13973	SWATH	CDK4_first_mutants	CDK4	WT	none	1	WT	13973_Cdk4wt_SLRIACG01_Swath.wiff	TrapElute-nanoflexSwath	1
13975	SWATH	CDK4_first_mutants	CDK4	WT	none	2	WT	13975_Cdk4wt_SLRIACG02_Swath.wiff	TrapElute-nanoflexSwath	1
13977	SWATH	CDK4_first_mutants	CDK4	WT	none	3	WT	13977_Cdk4wt_SLRIACG03_Swath.wiff	TrapElute-nanoflexSwath	1
14385	IDA	CDK4_expanded_mutants	CDK4	N41S	none	1	N41S	CDK4_a122g_mut_26JUL2012_BR1_IDA.wiff	PackedTipTop20	2
14379	IDA	CDK4_expanded_mutants	CDK4	R24C	none	4	R24C	CDK4_c70t_mut_26JUL2012_BR1_IDA.wiff	PackedTipTop20	2
14382	IDA	CDK4_expanded_mutants	CDK4	R24H	none	4	R24H	CDK4_g71a_mut_26JUL2012_BR1_IDA.wiff	PackedTipTop20	2
14388	IDA	CDK4_expanded_mutants	CDK4	S52N	none	1	S52N	CDK4_g155a_mut_26JUL2012_BR1_IDA_techrep1.wiff	PackedTipTop20	2
14376	IDA	CDK4_expanded_mutants	CDK4	WT	none	4	WT	CDK4_WT_26JUL2012_BR1_IDA.wiff	PackedTipTop20	2
14386	SWATH	CDK4_expanded_mutants	CDK4	N41S	none	1	N41S	CDK4_a122g_mut_26JUL2012_BR1_SWATH.wiff	PackedTipSwath	2
14387	SWATH	CDK4_expanded_mutants	CDK4	N41S	none	2	N41S	CDK4_a122g_mut_26JUL2012_BR2_SWATH.wiff	PackedTipSwath	2
14380	SWATH	CDK4_expanded_mutants	CDK4	R24C	none	4	R24C	CDK4_c70t_mut_26JUL2012_BR1_SWATH.wiff	PackedTipSwath	2
14381	SWATH	CDK4_expanded_mutants	CDK4	R24C	none	5	R24C	CDK4_c70t_mut_26JUL2012_BR2_SWATH.wiff	PackedTipSwath	2
14383	SWATH	CDK4_expanded_mutants	CDK4	R24H	none	4	R24H	CDK4_g71a_mut_26JUL2012_BR1_SWATH.wiff	PackedTipSwath	2
14384	SWATH	CDK4_expanded_mutants	CDK4	R24H	none	5	R24H	CDK4_g71a_mut_26JUL2012_BR2_SWATH.wiff	PackedTipSwath	2
14389	SWATH	CDK4_expanded_mutants	CDK4	S52N	none	1	S52N	CDK4_g155a_mut_26JUL2012_BR1_SWATH_techrep1.wiff	PackedTipSwath	2
14390	SWATH	CDK4_expanded_mutants	CDK4	S52N	none	2	S52N	CDK4_g155a_mut_26JUL2012_BR2_SWATH.wiff	PackedTipSwath	2
14377	SWATH	CDK4_expanded_mutants	CDK4	WT	none	4	WT	CDK4_WT_26JUL2012_BR1_SWATH.wiff	PackedTipSwath	2
14378	SWATH	CDK4_expanded_mutants	CDK4	WT	none	5	WT	CDK4_WT_26JUL2012_BR2_SWATH.wiff	PackedTipSwath	2
14014	IDA	CDK4_HSP90_inhibition	none	N/A	DMSO	1	FLAG_DMSO	14014_CDK_empty_BR1_DMSO_IDA.wiff	TrapElute-Nanoflex TOP20	3
14018	IDA	CDK4_HSP90_inhibition	none	N/A	NVP	1	FLAG_NVP	14018_CDK_empty_BR1_NVP_IDA.wiff	TrapElute-Nanoflex TOP20	3
13992	IDA	CDK4_HSP90_inhibition	CDK4	R24C	DMSO	1	R24C_DMSO	13992_CDK_c70t_BR1_DMSO_IDA.wiff	TrapElute-Nanoflex TOP20	3
13996	IDA	CDK4_HSP90_inhibition	CDK4	R24C	NVP	1	R24C_NVP	13996_CDK_c70t_BR1_NVP_IDA.wiff	TrapElute-Nanoflex TOP20	3
14006	IDA	CDK4_HSP90_inhibition	CDK4	R24H	DMSO	1	R24H_DMSO	14006_CDK_g71a_BR1_DMSO_IDA.wiff	TrapElute-Nanoflex TOP20	3
14010	IDA	CDK4_HSP90_inhibition	CDK4	R24H	NVP	1	R24H_NVP	14010_CDK_g71a_BR1_NVP_IDA.wiff	TrapElute-Nanoflex TOP20	3
13978	IDA	CDK4_HSP90_inhibition	CDK4	WT	DMSO	1	WT_DMSO	13978_CDK_WT_BR1_DMSO_IDA.wiff	TrapElute-Nanoflex TOP20	3
13982	IDA	CDK4_HSP90_inhibition	CDK4	WT	NVP	1	WT_NVP	13982_CDK_WT_BR1_NVP_IDA.wiff	TrapElute-Nanoflex TOP20	3
14015	SWATH	CDK4_HSP90_inhibition	none	N/A	DMSO	1	FLAG_DMSO	14015_CDK_empty_BR1_DMSO_SWATH.wiff	TrapElute-NanoflexSwath	3
14017	SWATH	CDK4_HSP90_inhibition	none	N/A	DMSO	2	FLAG_DMSO	14017_CDK_empty_BR2_DMSO_SWATH.wiff	TrapElute-NanoflexSwath	3
14019	SWATH	CDK4_HSP90_inhibition	none	N/A	NVP	1	FLAG_NVP	14019_CDK_empty_BR1_NVP_SWATH.wiff	TrapElute-NanoflexSwath	3
14021	SWATH	CDK4_HSP90_inhibition	none	N/A	NVP	2	FLAG_NVP	14021_CDK_empty_BR2_NVP_SWATH.wiff	TrapElute-NanoflexSwath	3
13993	SWATH	CDK4_HSP90_inhibition	CDK4	R24C	DMSO	1	R24C_DMSO	13993_CDK_c70t_BR1_DMSO_SWATH.wiff	TrapElute-NanoflexSwath	3
13995	SWATH	CDK4_HSP90_inhibition	CDK4	R24C	DMSO	2	R24C_DMSO	13995_CDK_c70t_BR2_DMSO_SWATH.wiff	TrapElute-NanoflexSwath	3
13997	SWATH	CDK4_HSP90_inhibition	CDK4	R24C	NVP	1	R24C_NVP	13997_CDK_c70t_BR1_NVP_SWATH.wiff	TrapElute-NanoflexSwath	3
13999	SWATH	CDK4_HSP90_inhibition	CDK4	R24C	NVP	2	R24C_NVP	13999_CDK_c70t_BR2_NVP_SWATH.wiff	TrapElute-NanoflexSwath	3
14007	SWATH	CDK4_HSP90_inhibition	CDK4	R24H	DMSO	1	R24H_DMSO	14007_CDK_g71a_BR1_DMSO_SWATH.wiff	TrapElute-NanoflexSwath	3
14009	SWATH	CDK4_HSP90_inhibition	CDK4	R24H	DMSO	2	R24H_DMSO	14009_CDK_g71a_BR2_DMSO_SWATH.wiff	TrapElute-NanoflexSwath	3
14011	SWATH	CDK4_HSP90_inhibition	CDK4	R24H	NVP	1	R24H_NVP	14011_CDK_g71a_BR1_NVP_SWATH.wiff	TrapElute-NanoflexSwath	3
14013	SWATH	CDK4_HSP90_inhibition	CDK4	R24H	NVP	2	R24H_NVP	14013_CDK_g71a_BR2_NVP_SWATH.wiff	TrapElute-NanoflexSwath	3
13979	SWATH	CDK4_HSP90_inhibition	CDK4	WT	DMSO	1	WT_DMSO	13979_CDK_WT_BR1_DMSO_SWATH.wiff	TrapElute-NanoflexSwath	3
13981	SWATH	CDK4_HSP90_inhibition	CDK4	WT	DMSO	2	WT_DMSO	13981_CDK_WT_BR2_DMSO_SWATH.wiff	TrapElute-NanoflexSwath	3
13983	SWATH	CDK4_HSP90_inhibition	CDK4	WT	NVP	1	WT_NVP	13983_CDK_WT_BR1_NVP_SWATH.wiff	TrapElute-NanoflexSwath	3
13985	SWATH	CDK4_HSP90_inhibition	CDK4	WT	NVP	2	WT_NVP	13985_CDK_WT_BR2_NVP_SWATH.wiff	TrapElute-NanoflexSwath	3
14200	IDA	GRK6_splice_variants	GRK6	A	none	4	GRK6_A	14200_GRK6_A_BR4_IDA.wiff	PackedTipTop10	4
14226	IDA	GRK6_splice_variants	GRK6	A	none	5	GRK6_A	14226_GRK6_A_BR5_IDA.wiff	PackedTipTop10	4
14202	IDA	GRK6_splice_variants	GRK6	B	none	4	GRK6_B	14202_GRK6_B_BR4_IDA.wiff	PackedTipTop10	4
14224	IDA	GRK6_splice_variants	GRK6	B	none	5	GRK6_B	14224_GRK6_B_BR5_IDA.wiff	PackedTipTop10	4
14205	IDA	GRK6_splice_variants	GRK6	C	none	4	GRK6_C	14204_GRK6_C_BR4_IDA.wiff	PackedTipTop10	4
14222	IDA	GRK6_splice_variants	GRK6	C	none	5	GRK6_C	14222_GRK6_C_BR5_IDA.wiff	PackedTipTop10	4
14445	SWATH	GRK6_splice_variants	GRK6	A	none	2	GRK6_A	AC_13842_GRK6_A_BR2_swath.wiff	PackedTipSwath	4
14453	SWATH	GRK6_splice_variants	GRK6	A	none	3	GRK6_A	13915_GRK6_A_BR3_swath.wiff	PackedTipSwath	4
14201	SWATH	GRK6_splice_variants	GRK6	A	none	4	GRK6_A	14201_GRK6_A_BR4_SWATH.wiff	PackedTipSwath	4
14227	SWATH	GRK6_splice_variants	GRK6	A	none	5	GRK6_A	14227_GRK6_A_BR5_SWATH.wiff	PackedTipSwath	4
14447	SWATH	GRK6_splice_variants	GRK6	B	none	2	GRK6_B	AC_13844_GRK6_B_BR2_swath.wiff	PackedTipSwath	4
14455	SWATH	GRK6_splice_variants	GRK6	B	none	3	GRK6_B	13917_GRK6_B_BR3_swath.wiff	PackedTipSwath	4
14203	SWATH	GRK6_splice_variants	GRK6	B	none	4	GRK6_B	14203_GRK6_B_BR4_SWATH.wiff	PackedTipSwath	4
14225	SWATH	GRK6_splice_variants	GRK6	B	none	5	GRK6_B	14225_GRK6_B_BR5_SWATH.wiff	PackedTipSwath	4
14449	SWATH	GRK6_splice_variants	GRK6	C	none	2	GRK6_C	AC_13846_GRK6_C_BR2_swath.wiff	PackedTipSwath	4
14451	SWATH	GRK6_splice_variants	GRK6	C	none	3	GRK6_C	13919_GRK6_C_BR3_swathrep.wiff	PackedTipSwath	4
14205	SWATH	GRK6_splice_variants	GRK6	C	none	4	GRK6_C	14205_GRK6_C_BR4_SWATH.wiff	PackedTipSwath	4
14223	SWATH	GRK6_splice_variants	GRK6	C	none	5	GRK6_C	14223_GRK6_C_BR5_SWATH.wiff	PackedTipSwath	4
16145	IDA	CDK4_triplicates	CDK4	R24C	none	6	R24C_9	16145_ZL_CDK4_C70T_BR1_IDA_TOF1chp_P36.wiff	TrapElute-nanoflexTop50	5
16212	IDA	CDK4_triplicates	CDK4	R24C	none	7	R24C_9	16212_ZL_CDK4_c70t_BR2_IDA_TOF1chp_P36.wiff	TrapElute-nanoflexTop50	5
16218	IDA	CDK4_triplicates	CDK4	R24C	none	8	R24C_9	16218_ZL_CDK4_c70t_BR3_IDA_TOF1chp_P36.wiff	TrapElute-nanoflexTop50	5
16147	IDA	CDK4_triplicates	CDK4	R24H	none	6	R24H_9	16147_ZL_CDK4_G71A_BR1_IDA_TOF1chp_P36.wiff	TrapElute-nanoflexTop50	5
16210	IDA	CDK4_triplicates	CDK4	R24H	none	7	R24H_9	16210_ZL_CDK4_G71A_BR2_IDA_TOF1chp_P36.wiff	TrapElute-nanoflexTop50	5
16214	IDA	CDK4_triplicates	CDK4	R24H	none	8	R24H_9	16214_ZL_CDK4_G71A_BR3_IDA_TOF1chp_P36.wiff	TrapElute-nanoflexTop50	5
16143	IDA	CDK4_triplicates	CDK4	WT	none	6	WT_9	16143_ZL_CDK4_WT_BR1_IDA_TOF1chp_P36.wiff	TrapElute-nanoflexTop50	5
16208	IDA	CDK4_triplicates	CDK4	WT	none	7	WT_9	16208_ZL_CDK4_WT_BR2_IDA_TOF1chp_P36.wiff	TrapElute-nanoflexTop50	5
16216	IDA	CDK4_triplicates	CDK4	WT	none	8	WT_9	16216_ZL_CDK4_WT_BR3_IDA_TOF1chp_P36.wiff	TrapElute-nanoflexTop50	5
16146	SWATH	CDK4_triplicates	CDK4	R24C	none	6.1	R24C_9	16146_ZL_CDK4_C70T_BR1_SWATH_TOF1chp_P36.wiff	TrapElute-nanoflexSwath	5
16499	SWATH	CDK4_triplicates	CDK4	R24C	none	6.2	R24C_9	16499_ZL_CDK4_c70t_BR1_2ndSWATH_TOF1chp_P36.wiff	TrapElute-nanoflexSwath	5
16500	SWATH	CDK4_triplicates	CDK4	R24C	none	6.3	R24C_9	16500_ZL_CDK4_c70t_BR1_3rdSWATH_TOF1chp_P36.wiff	TrapElute-nanoflexSwath	5
16213	SWATH	CDK4_triplicates	CDK4	R24C	none	7.1	R24C_9	16213_ZL_CDK4_c70t_BR2_SWATH_TOF1chp_P36.wiff	TrapElute-nanoflexSwath	5
16501	SWATH	CDK4_triplicates	CDK4	R24C	none	7.2	R24C_9	16501_ZL_CDK4_c70t_BR2_2ndSWATH_TOF1chp_P36.wiff	TrapElute-nanoflexSwath	5
16502	SWATH	CDK4_triplicates	CDK4	R24C	none	7.3	R24C_9	16502_ZL_CDK4_c70t_BR2_3rdSWATH_TOF1chp_P36.wiff	TrapElute-nanoflexSwath	5
16219	SWATH	CDK4_triplicates	CDK4	R24C	none	8.1	R24C_9	16219_ZL_CDK4_c70t_BR3_SWATH_TOF1chp_P36.wiff	TrapElute-nanoflexSwath	5
16503	SWATH	CDK4_triplicates	CDK4	R24C	none	8.2	R24C_9	16503_ZL_CDK4_c70t_BR3_2ndSWATH_TOF1chp_P36.wiff	TrapElute-nanoflexSwath	5
16504	SWATH	CDK4_triplicates	CDK4	R24C	none	8.3	R24C_9	16504_ZL_CDK4_c70t_BR3_3rdSWATH_TOF1chp_P36.wiff	TrapElute-nanoflexSwath	5

16148	SWATH	CDK4_triplicates	CDK4	R24H	none	6.1	R24H_9	16148_ZL_CDK4_G71A_BR1_SWATH_TOF1chp_P36.wiff	TrapElute-nanoflexSwath	5
16519	SWATH	CDK4_triplicates	CDK4	R24H	none	6.2	R24H_9	16519_ZL_CDK4_G71A_BR1_2ndSWATH_TOF1chp_P36.wiff	TrapElute-nanoflexSwath	5
16520	SWATH	CDK4_triplicates	CDK4	R24H	none	6.3	R24H_9	16520_ZL_CDK4_G71A_BR1_3rdSWATH_TOF1chp_P36.wiff	TrapElute-nanoflexSwath	5
16211	SWATH	CDK4_triplicates	CDK4	R24H	none	7.1	R24H_9	16211_ZL_CDK4_G71A_BR2_SWATH_TOF1chp_P36.wiff	TrapElute-nanoflexSwath	5
16521	SWATH	CDK4_triplicates	CDK4	R24H	none	7.2	R24H_9	16521_ZL_CDK4_G71A_BR2_2ndSWATH_TOF1chp_P36.wiff	TrapElute-nanoflexSwath	5
16522	SWATH	CDK4_triplicates	CDK4	R24H	none	7.3	R24H_9	16522_ZL_CDK4_G71A_BR2_3rdSWATH_TOF1chp_P36.wiff	TrapElute-nanoflexSwath	5
16215	SWATH	CDK4_triplicates	CDK4	R24H	none	8.1	R24H_9	16215_ZL_CDK4_G71A_BR3_SWATH_TOF1chp_P36.wiff	TrapElute-nanoflexSwath	5
16523	SWATH	CDK4_triplicates	CDK4	R24H	none	8.2	R24H_9	16523_ZL_CDK4_G71A_BR3_2ndSWATH_TOF1chp_P36.wiff	TrapElute-nanoflexSwath	5
16524	SWATH	CDK4_triplicates	CDK4	R24H	none	8.3	R24H_9	16524_ZL_CDK4_G71A_BR3_3rdSWATH_TOF1chp_P36.wiff	TrapElute-nanoflexSwath	5
16144	SWATH	CDK4_triplicates	CDK4	WT	none	6.1	WT_9	16144_ZL_CDK4_WT_BR1_SWATH_TOF1chp_P36.wiff	TrapElute-nanoflexSwath	5
16489	SWATH	CDK4_triplicates	CDK4	WT	none	6.2	WT_9	16489_ZL_CDK4_WT_BR1_2ndSWATH_TOF1chp_P36.wiff	TrapElute-nanoflexSwath	5
16490	SWATH	CDK4_triplicates	CDK4	WT	none	6.3	WT_9	16490_ZL_CDK4_WT_BR1_3rdSWATH_TOF1chp_P36.wiff	TrapElute-nanoflexSwath	5
16209	SWATH	CDK4_triplicates	CDK4	WT	none	7.1	WT_9	16209_ZL_CDK4_WT_BR2_SWATH_TOF1chp_P36.wiff	TrapElute-nanoflexSwath	5
16491	SWATH	CDK4_triplicates	CDK4	WT	none	7.2	WT_9	16491_ZL_CDK4_WT_BR2_2ndSWATH_TOF1chp_P36.wiff	TrapElute-nanoflexSwath	5
16492	SWATH	CDK4_triplicates	CDK4	WT	none	7.3	WT_9	16492_ZL_CDK4_WT_BR2_3rdSWATH_TOF1chp_P36.wiff	TrapElute-nanoflexSwath	5
16217	SWATH	CDK4_triplicates	CDK4	WT	none	8.1	WT_9	16217_ZL_CDK4_WT_BR3_SWATH_TOF1chp_P36.wiff	TrapElute-nanoflexSwath	5
16493	SWATH	CDK4_triplicates	CDK4	WT	none	8.2	WT_9	16493_ZL_CDK4_WT_BR3_2ndSWATH_TOF1chp_P36.wiff	TrapElute-nanoflexSwath	5
16494	SWATH	CDK4_triplicates	CDK4	WT	none	8.3	WT_9	16494_ZL_CDK4_WT_BR3_3rdSWATH_TOF1chp_P36.wiff	TrapElute-nanoflexSwath	5
17327	IDA	MEPCE_EIF4A2	GFP	N/A	none	1	GFP_1	IDA_GFPJune7-Biorep1.wiff	TrapElute-Nanoflex TOP20	6
17328	IDA	MEPCE_EIF4A2	GFP	N/A	none	2	GFP_2	IDA_GFPJune7-Biorep2.wiff	TrapElute-Nanoflex TOP20	6
17329	IDA	MEPCE_EIF4A2	GFP	N/A	none	3	GFP_3	IDA_GFPJune7-Biorep3.wiff	TrapElute-Nanoflex TOP20	6
17571	IDA	MEPCE_EIF4A2	EIF4A2	WT	none	1	EIF4A2_1	IDA_EIF4aJune7-Biorep1.wiff	TrapElute-Nanoflex TOP20	6
17315	IDA	MEPCE_EIF4A2	MEPCE	WT	none	1	MEPCE_1	IDA_MEPCEJune7-Biorep1.wiff	TrapElute-Nanoflex TOP20	6
17572	IDA	MEPCE_EIF4A2	EIF4A2	WT	none	2	EIF4A2_2	IDA_EIF4aJune7-Biorep2.wiff	TrapElute-Nanoflex TOP20	6
17316	IDA	MEPCE_EIF4A2	MEPCE	WT	none	2	MEPCE_2	IDA_MEPCEJune7-Biorep2.wiff	TrapElute-Nanoflex TOP20	6
17573	IDA	MEPCE_EIF4A2	EIF4A2	WT	none	3	EIF4A2_3	IDA_EIF4aJune7-Biorep3.wiff	TrapElute-Nanoflex TOP20	6
17317	IDA	MEPCE_EIF4A2	MEPCE	WT	none	3	MEPCE_3	IDA_MEPCEJune7-Biorep3.wiff	TrapElute-Nanoflex TOP20	6
17330	SWATH	MEPCE_EIF4A2	GFP	N/A	none	1	GFP_1	Swath_GFPJune7-Biorep1.wiff	TrapElute-nanoflexSwath	6
17331	SWATH	MEPCE_EIF4A2	GFP	N/A	none	2	GFP_2	Swath_GFPJune7-Biorep2.wiff	TrapElute-nanoflexSwath	6
17332	SWATH	MEPCE_EIF4A2	GFP	N/A	none	3	GFP_3	Swath_GFPJune7-Biorep3.wiff	TrapElute-nanoflexSwath	6
17574	SWATH	MEPCE_EIF4A2	EIF4A2	WT	none	1	EIF4A2_1	Swath_EIFraJune7-Biorep1.wiff	TrapElute-nanoflexSwath	6
17318	SWATH	MEPCE_EIF4A2	MEPCE	WT	none	1	MEPCE_1	Swath_MEPCEJune7-Biorep1.wiff	TrapElute-nanoflexSwath	6
17575	SWATH	MEPCE_EIF4A2	EIF4A2	WT	none	2	EIF4A2_2	Swath_EIF4aJune7-Biorep2.wiff	TrapElute-nanoflexSwath	6
17319	SWATH	MEPCE_EIF4A2	MEPCE	WT	none	2	MEPCE_2	Swath_MEPCEJune7-Biorep2b.wiff	TrapElute-nanoflexSwath	6
17575	SWATH	MEPCE_EIF4A2	EIF4A2	WT	none	3	EIF4A2_3	Swath_EIF4aJune7-Biorep3.wiff	TrapElute-nanoflexSwath	6
17320	SWATH	MEPCE_EIF4A2	MEPCE	WT	none	3	MEPCE_3	Swath_MEPCEJune7-Biorep3.wiff	TrapElute-nanoflexSwath	6
17302	IDA-iTRAQ	CDK4_iTRAQ	CDK4	mixed	none	1	CDK4_iTRAQ_1	17302_CDK4_iTRAQ_BR1_TOF3_06JUN2013_IDA.wiff	PackedTip-iTRAQ	7
17303	IDA-iTRAQ	CDK4_iTRAQ	CDK4	mixed	none	2	CDK4_iTRAQ_2	17303_CDK4_iTRAQ_BR2_TOF3_06JUN2013_IDA.wiff	PackedTip-iTRAQ	7
17304	IDA-iTRAQ	CDK4_iTRAQ	CDK4	mixed	none	3	CDK4_iTRAQ_3	17304_CDK4_iTRAQ_BR3_TOF3_06JUN2013_IDA.wiff	PackedTip-iTRAQ	7

Supplementary Table 3. List the antibodies used in this study. Suppliers, catalog number and dilution used here are listed.

Antibody	Supplier	Product #	Dilution
Anti-FLAG M2 antibody	SIGMA	F1804	1:5000
Anti-CDK4 antibody	Cell Signaling Technology	#2906	1:5000
Anti-CDKN2C antibody	Cell Signaling Technology	#2896	1:1000
Anti-CCND3 antibody	Cell Signaling Technology	#2936	1:1000
Anti-CDN1B antibody	Cell Signaling Technology	#2552	1:1000
Anti-CCND1 antibody	Cell Signaling Technology	#2926	1:1000
Anti-HSP90α/β antibody	Santa Cruz Biotechnology	sc-7947	1:1000
Anti-CDC37 antibody	Santa Cruz Biotechnology	sc-17758	1:1000
Anti-CRKL antibody	Santa Cruz Biotechnology	sc-319	1:1000
Anti-FKBP5	Bethyl Laboratories	A301-430A	1:2500
Anti-tubulin	DSHB at the University if Iowa	E7	1:5000
IRDye® 800CW anti-mouse	Mandel	926-32210	1:10000
IRDye® 680 anti-rabbit	Mandel	926-32221	1:10000

Supplementary Table 4. Access to mass spectrometry files generated in this study deposited at MassiVE

Short experiment descriptor	Group file	ProHits export ID	MassIVE ID	MassiVE link for download
APSWATH_CDK4_original_set	1	P93_VS6	MSV000078453	http://massive.ucsd.edu/ProteoSAFe/status.jsp?task=1458cbae250748b18fea56e5d77cbcea
APSWATH_CDK4_expanded_mutants_set	2	P93_VS7	MSV000078455	http://massive.ucsd.edu/ProteoSAFe/status.jsp?task=39ad1793361c462c8ff94d2c9532ab9c
APSWATH_CDK4_NVP_set	3	P93_VS5	MSV000078456	http://massive.ucsd.edu/ProteoSAFe/status.jsp?task=37017e38bb684c02bf36f7ad6ff2e215
APSWATH_GRK6_set	4	P93_VS4	MSV000078457	http://massive.ucsd.edu/ProteoSAFe/status.jsp?task=3ae53e1cbead4ac687e54ea529099218
APSWATH_CDK4_triplicates_set	5	P93_VS3	MSV000078458	http://massive.ucsd.edu/ProteoSAFe/status.jsp?task=ccc883335df94b98910829655d92a6d0
APSWATH_MEPCE_EIF4A2_set	6	P94_VS1	MSV000078454	http://massive.ucsd.edu/ProteoSAFe/status.jsp?task=442926e304aa43158891b3318fa1993d
APSWATH_CDK4_iTRAQ_set	7	P93_VS8	MSV000078459	http://massive.ucsd.edu/ProteoSAFe/status.jsp?task=83d381369e3f42d789b0ef520ca7ea38